

We are IntechOpen, the world's leading publisher of Open Access books Built by scientists, for scientists

4,800

Open access books available

122,000

International authors and editors

135M

Downloads

Our authors are among the

154

Countries delivered to

TOP 1%

most cited scientists

12.2%

Contributors from top 500 universities



WEB OF SCIENCE™

Selection of our books indexed in the Book Citation Index
in Web of Science™ Core Collection (BKCI)

Interested in publishing with us?
Contact book.department@intechopen.com

Numbers displayed above are based on latest data collected.
For more information visit www.intechopen.com



Prostate

Ragab Hani Donkol¹ and Ahmad Al Nammi²

¹*Cairo University*

²*Aseer Central Hospital*

¹*Egypt*

²*Saudi Arabia*

1. Introduction

The value of prostatic sonography has dramatically increased in the past three decades. Transrectal ultrasound (TRUS) imaging is currently an integral part of prostate cancer diagnosis and treatment procedures, providing high-resolution anatomical detail of the prostate region. In this chapter we review the anatomy and sonographic methods in imaging of the prostate and prostatic diseases. Also we emphasize the role of new sonographic techniques, such as color and power Doppler, the use of contrast agents, 3D sonography and elastography for diagnosis of different prostate diseases especially prostate cancer. We also discuss the use of systematic and targeted sonographic-guided biopsies as gold standard for prostate cancer detection. Finally, we will elaborate the new role of ultrasound in management of prostate cancer.

2. Anatomy of the prostate

2.1 Embryology of the prostate

In the 4th week of gestation, the urogenital septum divides the cloaca into two parts: The rectum posteriorly and the primitive urogenital sinus anteriorly. In the 5th week, the distal portions of the Wolffian canal and the Mullerian canal attach to the posterior aspect of the primitive urogenital sinus (Fig. 1) to form an elevation called Mullerian tubercle. The tubercle divides the primitive urogenital sinus into vesico-urethral canal superiorly and definitive urogenital sinus inferiorly. The Wolffian canal forms the vas deferens, the ampulla of the vas and the seminal vesicle. The Mullerian canal regresses to form the utricule. Formation of the prostate begins at the 10th week of gestation by proliferation of the epithelium of the posterior urethra around the orifices of the Wolffian canal, to surround the urethral circumference. The prostatic glands formed anterior to the urethra regress and are replaced by fibromuscular stroma. The secretory function of the glands starts about the 13th week of gestation. (Brandes, 1989).

2.2 Gross anatomy of the prostate and its relations

The term “prostate” was originally derived from the Greek word “prohistani”, meaning “to stand in front”, and has been used to describe the organ located in front of the urinary bladder (Lowsley, 1912). The prostate is conical in shape with its long axis directed

inferiorly and anteriorly. The shape and size of the prostate may vary with age. The prostate of an adult man measures 20 – 25 gms in weight. The base of the prostate is directed superiorly and in contact with the bladder base. The apex is directed inferiorly and in contact with the external sphincter above the deep fascia of the urogenital membrane. The anterior border is separated from the symphysis pubis and pubic bones by the retropubic space which contains loose areolar tissue, preprostatic venous plexus, lymphatics, nerves and puboprostatic ligament. The trapezoid area is an extraprostatic area of anatomic weakness. It may be involved by carcinoma extending through the inferior neurovascular pedicle. This area bounded by the prostate proximally, the rectourethralis muscle distally, the membranous urethra anteriorly and the rectum posteriorly (Mayers et al, 1987). Posteriorly, the prostate is related to the rectum and is separated from it by the Denoviller's fascia which extends superiorly, behind the seminal vesicles up to the peritoneal reflection. At each posterolateral aspect of the prostate, the hypogastric pelvic fascia contains the neurovascular bundle of the prostate, seminal vesicles and bladder neck (Fig. 2).

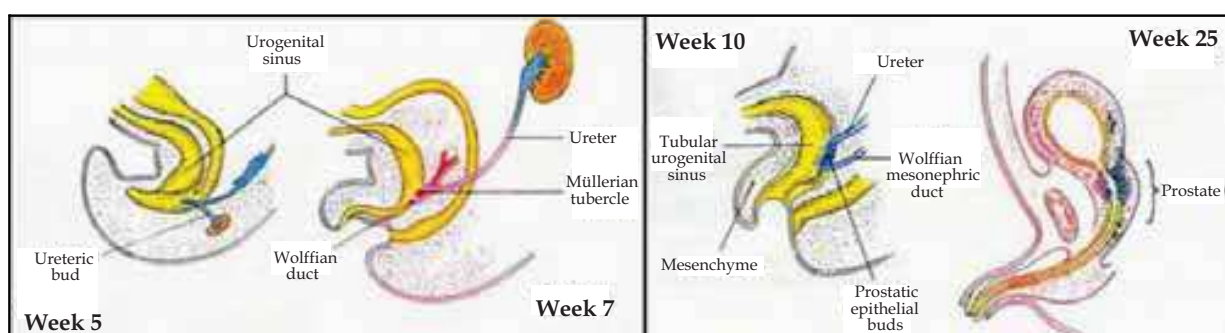


Fig. 1. The embryological origin and development of the prostatic urethra and the prostate (adapted from Delmas, 1991)

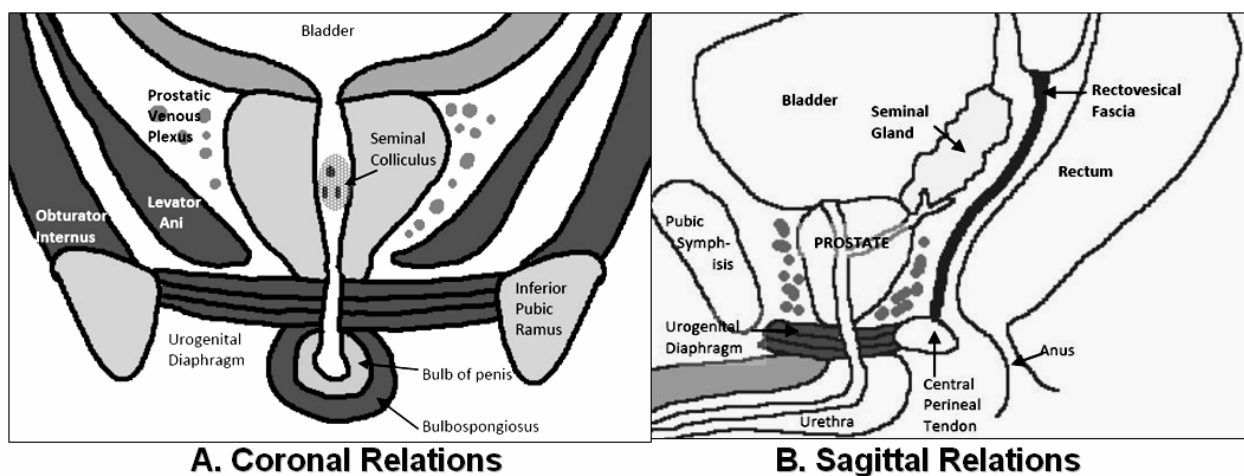


Fig. 2. Relations of the prostate in the coronal (A) and sagittal planes (B)

2.3 The distal seminal tract

It is formed of two seminal vesicles, ampullae of the vasa deferentia and ejaculatory ducts. The seminal vesicle is a cystic structure, measuring about 35 mm in length and 15 mm in width. It is related anteriorly to the urinary bladder and posteriorly to the the rectum. The ampula of the vas is located medial to the seminal vesicle. The vassal ampula joins the

seminal vesicle to form the ejaculatory duct. Each duct enters the base of the prostate, passes through central zone to end in the urethra below the utricle (Brandes, 1989).

2.4 Lobar concept of intraprostatic anatomy

In 1912, Lowsley demonstrated the first detailed description of the anatomy of the prostate. This traditional concept which is no longer used, divided the prostate into lobes: an anterior, posterior, middle and two lateral lobes. This method has been used to identify the prostate and prostatic disease for about 60 years. The anterior lobe was situated from the anterior margin of the gland to the level of the prostatic urethra. The middle lobe was a small area between the proximal prostatic urethra and the ejaculatory ducts. This lobe extends from the base of the prostate to the level of verumontanum. The posterior lobe was situated posterior to the ejaculatory ducts and extends to the posterior margin of the gland. The two lateral lobes extend from the lateral margin of the gland bilaterally toward the middle part of the gland. None of these lobes has clearly defined medial margin (Lowsley, 1912).

2.5 Zonal concept of intraprostatic anatomy

The understanding of the gross and microscopic anatomy of the prostate has changed during the past few decades. Since 1965, a zonal concept of anatomy has evolved initially developed by McNeal and then modified over about three decades. The prostate is best considered to be a fusion of different glandular regions contained within a discontinuous capsule (McNeal, 1968, 1988). The prostate is composed of four glandular regions and a non-glandular region which is the anterior fibromuscular stroma (Fig. 3). The fibromuscular stroma (FMS) is the anteromedial portion of the gland is devoid of glandular tissue. This region is generally considered to be of less clinical significance. The peripheral zone (PZ) comprises the largest portion of the glandular prostate in young man (70%). The PZ is

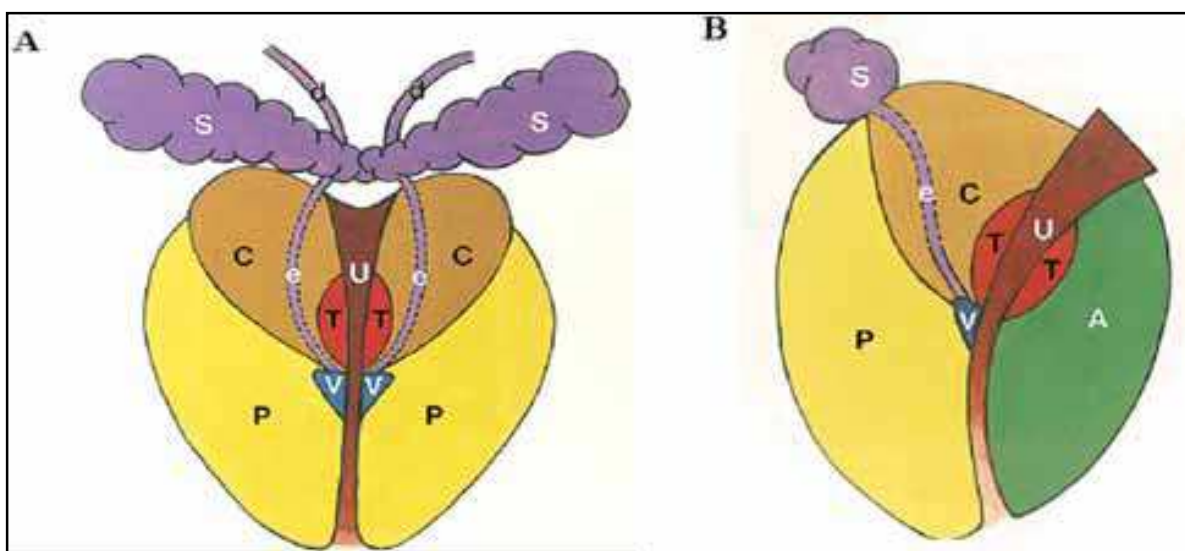


Fig. 3. Zonal anatomy of the prostate in coronal and sagittal planes showing the central zone (C), peripheral zone (P), transition zone (T) and anterior fibromuscular stroma (A). It also shows the distal seminal tract formed of the ampulla of the vas deference (d) which joins the seminal vesicle (S) to form ejaculatory duct (e) which opens at vera montanum (v) (adapted from McNeal 1968)

situated posteriorly, posterolaterally and a thin layer of this tissue also extends up laterally and anterolaterally. Distal to the verumontanum, the PZ often surrounds the urethra and occupies the apical region of the prostate. The transition zone (TZ) is situated on both sides of the proximal prostatic urethra and comprises only 5 to 10% of the glandular tissue in the non hyperplastic prostate. The surgical capsule is an interface between the PZ and TZ. In the aging prostate where the TZ can show marked glandular hyperplasia and may constitute the majority of prostatic glandular elements. The periurethral glandular zone (PUG) consists of mucosal glands in the prostatic urethra itself and represents only a tiny fraction of the glandular prostate. This zone may become hyperplastic with age to form the “median lobe” which may obstruct the bladder neck. The central zone (CZ) is cone-shaped with its base forms the base of prostate, bordering the urinary bladder and seminal vesicles and its apex is at the verumontanum. The CZ forms about 25% of the glandular prostatic tissue. The CZ surrounds the ejaculatory ducts throughout their entire courses in the prostate. The site where the ejaculatory ducts enter the CZ is devoid of prostatic capsule. The extraprostatic space invaginates around the ejaculatory ducts down to the verumontanum forming the “invaginated extra prostatic space”. If the ejaculatory ducts are invaded by carcinoma, the tumor will have a ready “highway” to the seminal vesicles and extraprostatic space.

2.6 Correlation of the lobar and zonal concepts of anatomy of the prostate

A comparison of Lowsley lobar and McNeal zonal concepts of anatomy is possible and important to compare the clinical findings. Clinicians may still refer to lobar anatomy while radiologists use zonal anatomy. So, the anterior lobe correlates with the anterior fibromuscular stroma. The medial lobe and the CZ are similar. The sum of the posterior and two lateral lobes correlated to a large extent with the PZ.

2.7 Correlation of the zonal anatomy and origin of prostatic diseases

With the development of cross sectional – imaging studies like transrectal ultrasound (TRUS) and magnetic resonance imaging (MRI), the zonal concept of anatomy becomes useful technique to apply because the different areas can be definite (Rifkin et al, 1990). The zonal concept of anatomy is also useful because it incorporated a clearer understanding of the development of disease. The origin of prostatic disease was poorly understood under Lowsley’s concept of lobar anatomy. It was previously thought that cancer only arises in the posterior lobe and BPH develops predominantly in the lateral and, to a lesser degree in the median lobe. It is now understood that the prostate cancer develops in the acinar tissue predominantly the peripheral prostate. Although the PZ is three times larger in volume than the CZ, prostate cancer develops seven times more often in the PZ. It was shown that about 50% of cancer arises in the anterior half of the prostate, including all those cancers from the TZ (20% of the total), CZ (10%) and anteriorly situated portions of the PZ. In contrast, BPH develops exclusively from the central gland, approximately 95% from the TZ and 5% from the periurethral glandular tissue. Prostatitis (when not due to surgical manipulation) starts mainly in the PZ similar to the prostatic cancer (McNeal et al 1988).

3. Techniques and approaches of prostatic ultrasonography

Ultrasonography is firmly established diagnostic tool in prostatic imaging. Recent development in US technology has led to significant improvements in image quality,

consistency and resolution. Additionally, dynamic scanners, color flow imaging and real time imaging have allowed appreciation of blood flow, reduced examination time and improved quality of the image. These advances combined with the portability, relative low cost and lack of risks of iodinated contrast media and irradiation have made US one of the most useful modality in evaluation of the prostate. Many approaches can be used to image the prostate as trans-abdominal, trans-urethral, trans-perineal and transrectal US. The common two approaches are transabdominal and transrectal ultrasound.

3.1 Trans-abdominal ultrasound

Transabdominal US of the prostate is nearly universally available and provides excellent anatomic information using the urine-filled bladder as an acoustic window. Prostate size, weight, shape and intravesical extent can be determined. Caudal angulation of the transducer to accommodate the pubic bone is often required. The normal prostate appears as a homogenous, round or ovoid structure with uniform low level echoes. The intraglandular zonal anatomy can not be visualized (Fig. 4). The relation between the prostate, bladder and seminal vesicles can be demonstrated (Abu-Yosef & Noryana 1982).

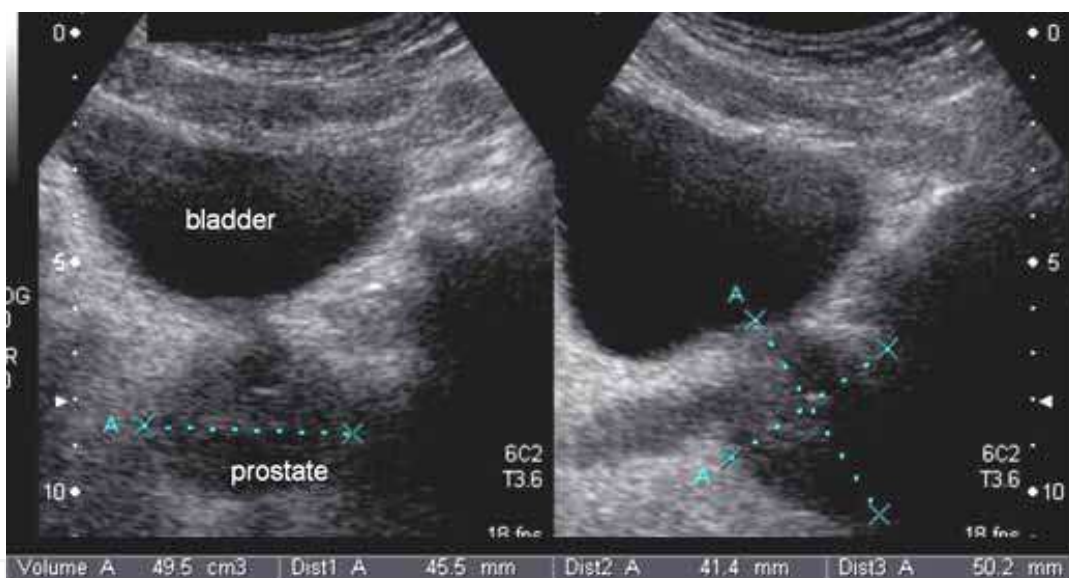


Fig. 4. Transabdominal US of a moderately enlarged prostate in axial and sagittal planes

3.2 Transrectal ultrasound (TRUS)

In 1963, Takahashi and Ouchi were the first to describe the use of TRUS to evaluate the prostate. The first clinically applicable images of the prostate obtained with TRUS were described in 1967 by Watanabe et al, they used a 3.5 MHz transducer, which at that time was considered to be state of the art, to obtain images that were clinically meaningful. As US technology has become more refined, the use of TRUS in the evaluation of prostatic disease has increased. By the mid 1980s, TRUS had become a standard diagnostic instrument of the urologists and radiologists. Most investigators today prefer equipment using hand-held transducers which are available in frequencies ranging from 3.5 MHz up to 10 MHz with the optimum frequency being around 7.0 MHz. Transrectal probes are available in different sizes and shapes with diameters ranging from 1.2 to 2 cm.

4. Sonographic anatomy of the normal prostate

Transrectal US of the prostate has revolutionized our ability to examine this organ. It provides excellent visualization of the prostate in the axial and sagittal planes.

In the axial plane, scanning usually begins at a level just above the seminal vesicles and by sequential withdrawing of the transducer in a caudal direction, the base, mid gland and the apex is visualized (Fig. 5). When scanning the most cephalad areas, the vas deferens will be visualized. They will appear as bilateral round cystic structures. Then the seminal vesicles will come into view as the vas deferens joins with them superior to the prostate. They usually appear as bow-tie configuration, but they may be rounded, lobulated or flattened. At the level of the base of the prostate, the prostate appears as a symmetrical crescent-shaped with triangular postero-lateral margin. The normal prostate will appear hyperechoic to the seminal vesicles and will have a homogenous echopattern. The CZ and TZ cannot be individually distinguished by their echogenicity. However the PZ appears more echogenic with homogenous echotexture. At the level of mid gland, the prostate becomes ovoid in shape. The anterior fibromuscular tissue is seen and has an echogenicity equal to or less than that of the glandular areas. The hypoechoic periurethral glandular tissue is demonstrated as hypoechoic area in the midline. Posterior and lateral to the PUG tissue, the PZ appears more echogenic and homogenous. The apex of the prostate appears more rounded. The obturator internus and levator ani muscles appear as hyperechoic structures lateral to the prostate apex. The prostate is surrounded by hyperechoic layer comprising the prostatic capsule and surrounding fat and fascia. The normal prostatic urethra is rarely visualized. The advantages of axial scanning include visualization of the left-right symmetry and echotexture, visualization of the anterior lateral portions of the PZ in a single view and assessment the lateral extracapsular spread of carcinoma (Rifkin, 1997).

In the sagittal plane scanning starts in the midline where the entire prostate can be visualized in one image. The seminal vesicle will be superior and posterior to the base of the prostate, and the vas deferens will be seen anterior to the seminal vesicles. The seminal vesicles will be less echogenic than the prostate and will appear rounded in shape. In the midline sagittal plane, the hypoechoic periurethral tissue will be seen and may be difficult to differentiate from the anterior fibromuscular stroma. The rest of the prostate will be homogenous in echogenicity with the PZ slightly more echogenic than the CZ and TZ (fig. 6). By tilting the transducer slightly to the right or the left of midline, the lateral aspects of the prostate and seminal vesicles will be visualized. The lateral aspects of the prostate are normally more rounded and homogenous in echogenicity. The ejaculatory ducts can be identified as hypoechoic line structures between two parallel echogenic lines as the course from the seminal vesicles through the CZ into prostatic urethra. The advantages of sagittal scanning include evaluation of the base and apex of the prostate in a single view, accurate measurement of the cranio-caudal diameter of the prostate or of a lesion within the prostate and better demonstration of the prostatic urethra and ejaculatory ducts ((Rifkin, 1997)

Estimation of prostate volume may be useful in a variety of clinical settings. In cases of BPH, most urologists prefer to perform transurethral resections for glands under 60 grams, while open prostatectomy is preferred for glands over 60 grams (Narayan & Foster 1991). Other potential users include the comparison of the prostate volume with levels of PSA for early detection of the prostatic cancer. PSA density is an index calculated by dividing PSA by the volume of the prostate measured by TRUS. In absence of cancer, prostatic volume is directly

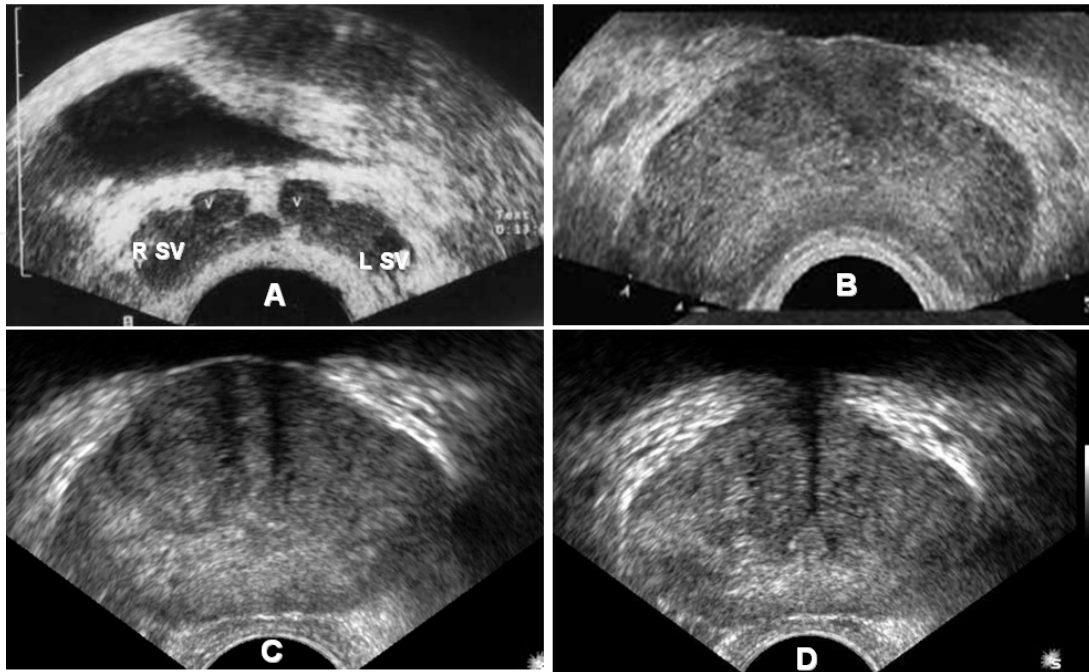


Fig. 5. TRUS axial images. (A) the level of distal seminal tract; showing seminal vesicle (SV) and vasl ampulla (V), (B) level of prostate base, (C) level of mid gland and (D) level of vera montanum showing its appearance as tour Eiffel

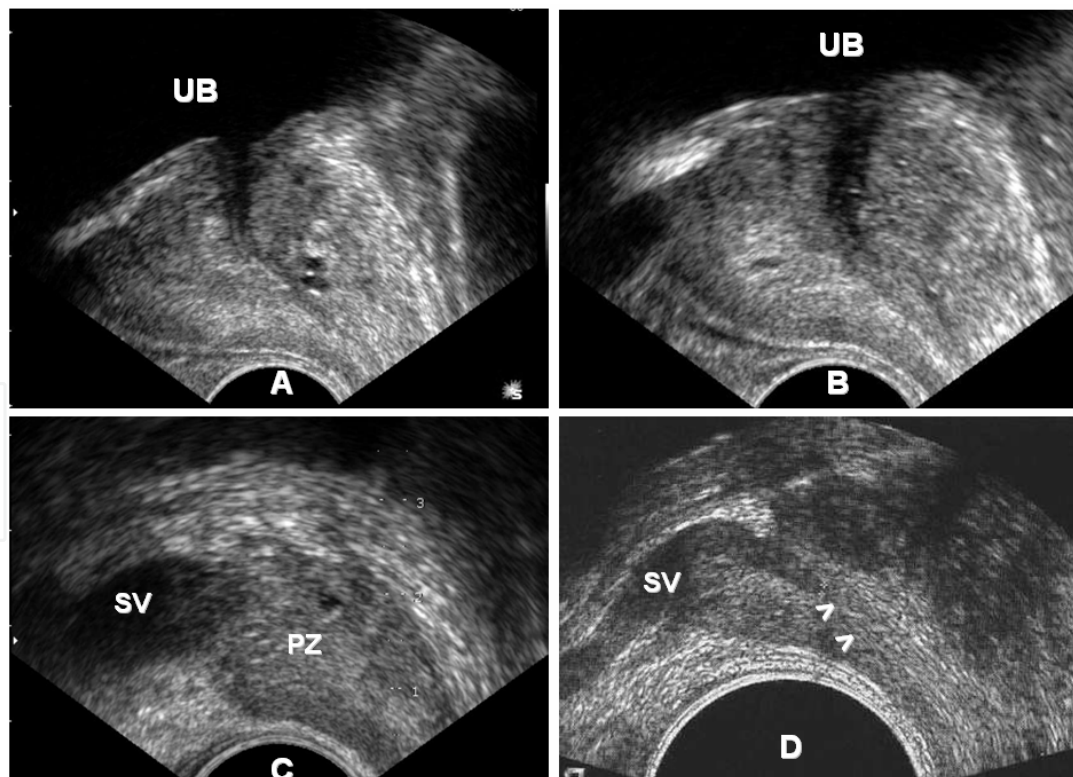


Fig. 6. TRUS sagittal images; (A) in midline; (B) in paramedical region; (C) peripheral part of the gland which is formed mainly of peripheral zone (PZ) and above it the body of seminal vesicle (SV) and (D) shows the confluence of vas and seminal vesicle (SV) to form the ejaculatory duct (arrowhead)

proportional to circulating serum PSA (Benson et al., 1992). Benign prostatic hyperplasia is associated with, on average, only 0.26 ng/mL PSA per gram of tissue, whereas cancer results in a density 10-fold higher (Hammerer et al., 1995). Any PSA value greater than that predicted by gland volume should raise a suspicion of prostate cancer. Also, the pre-treatment estimation of the volume of prostate cancer can provide important prognostic information after hormonal or radiation therapy. (Terris & Stamey 1991). The commonly used method in measuring prostate volume is the elliptical method. This formula can be transformed into $\text{volume} = 0.523 \times d_1 \times d_2 \times d_3$. Maximal width and height diameters are obtained at the largest appearing mid gland axial image section. The length dimension can be obtained on midline sagittal plane (Fig. 9). This method is widely used because it is easy and fast method. The fact that it is slightly less accurate than other methods is not documented (Terris & Stamey, 1990).

5. Diseases of the prostate and their sonographic appearance

5.1 Cysts of the prostate

Cysts of the prostate are confusing abnormalities because they are uncommon and their origin is uncertain. Small cysts are asymptomatic while large cysts may present with symptoms of urinary tract irritation, obstruction or hypofertility. The cysts may be complicated by infection, and stone formation. They may be turned malignant in about 3% of cases (Litirup et al., 1988). The cysts are usually unilocular, sharply defined, thin walled and anechoic. They vary size from 0.5 cm to 3.0 cm in diameters (Fig. 7). Prostatic cysts are either midline prostatic cysts like utricle cyst and Mullerian duct cyst or lateral prostatic cysts as cysts of the ejaculatory ducts or acquired cysts which are associated with prostate cancer, PBH, and prostatic abscess (Patel et al., 2002). Utricle cysts are dilatation of the prostatic utricle which may be congenital (megautricle) or acquired due to obstruction of its orifice by inflammation (utriclocele). The utricle cysts are small intraprostatic midline cysts. Mullerian duct cysts are remnants of Mullerian duct. These cysts are relatively large, extends superiorly and inferiorly from the level of the verumontanum even outside the prostate. Ejaculatory ducts cysts are present along the course of the ejaculatory ducts within the CZ. They are usually paramedian and unilateral. They are complex cysts with solid and cystic components. They containing spermatozoa. Extra-prostatic cysts are either cysts of the seminal vesicles or the ampulae of the vas. They are congenital in origin and associated with urinary tract anomalies. Some patients are manifested by obstructive azospermia and TRUS can classify the patients without cysts where TRUS-guided aspiration and seminal vesiculography can be performed and patients with cyst where TRUS-guided cyst aspiration and opacification can be performed (Donkol, 2010).

5.2 Inflammatory diseases the prostate

Acute prostatitis is acute bacterial inflammation of the prostate. The clinical diagnosis usually is not difficult. The patient has fever, perineal and low back pain; pain with defecation of after ejaculation; urethral discharge associated with dysuria, urgency, frequency, or retention. On examination, the prostate is swollen, boggy and tender. Griffiths and associates in 1984 described three characteristic sonographic features seen in a group of 40 patients with an acute inflammation of the prostate as a periurethral echo-poor halo, a

prominent periprostatic venous plexus and hypoechoic areas within the prostate, predominantly in the peripheral zone (Griffiths et al., 1984).

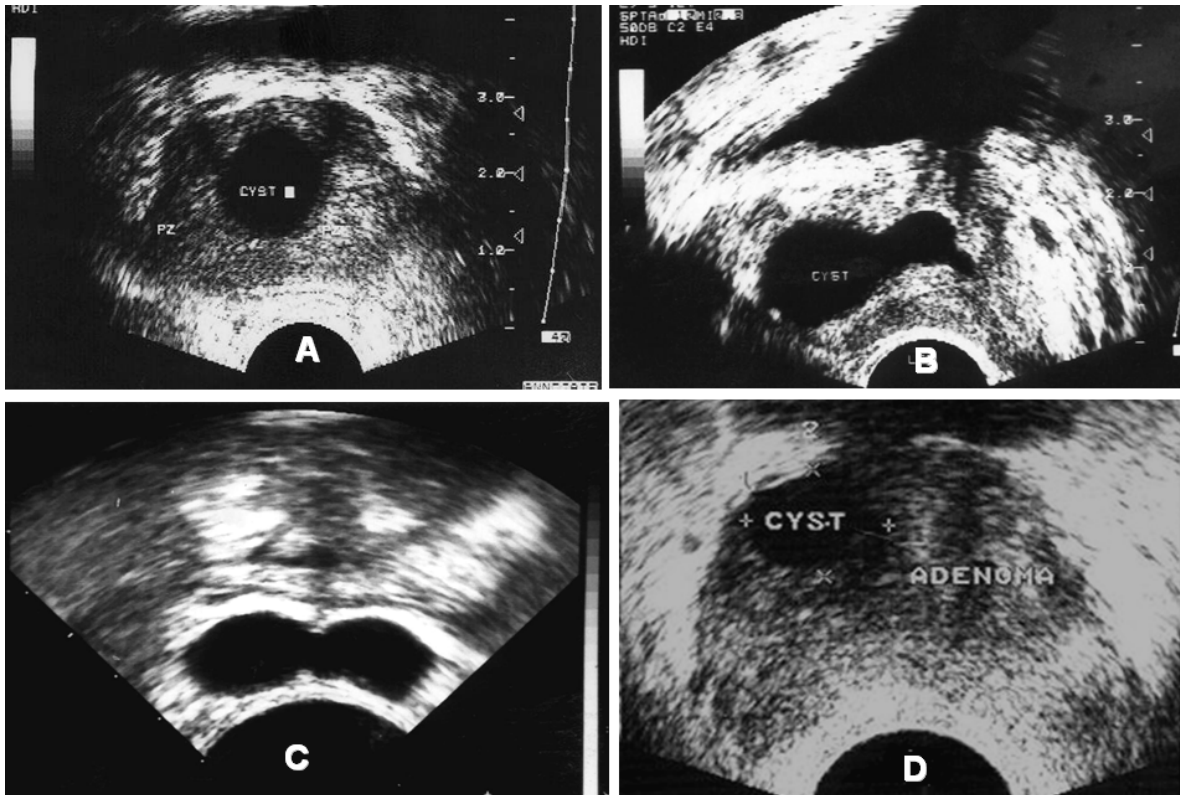


Fig. 7. TRUS of different prostatic cysts. (A) Axial TRUS of a utricle cyst; the cyst is midline and intraprostatic. (B) Sagittal TRUS of Mullerian duct cyst; the cyst is midline is midline with supraprostatic extension. (C) Axial TRUS of bilateral seminal vesicles cysts in a patient with obstructive azospermia. (D) Axial TRUS shows an acquired intraprostatic cyst in the in the right part of adenoma of benign prostatic hypertrophy

Chronic prostatitis may be infective as a complication of acute prostatitis or noninfective secondary to congestion of the prostate or urinary reflux into the prostate resulting in inflammatory or fibrotic reaction or both within the prostate. Chronic prostatitis has varied symptomatology and lack of physical signs. The diagnosis currently rests on the finding of excessive leukocytes in prostatic secretions. Sonographic findings include high density echoes, mid range echoes, echo-lucent zones, ejaculatory duct calcifications, capsular irregularity, capsular thickening and periurethral zone irregularity (Fig. 8 A&B). The sensitivity and specificity of these signs are low (Doble & Carter, 1989)

Prostatic abscesses have been reported in an older age group due bladder outlet obstruction and urinary tract infection. Iatrogenic prostatic abscess have been reported after biopsy or instrumentation. Half of the patients presenting in acute retention and half presenting with irritative voiding symptoms. Of the patients 40% have fever, 25% have associated epididymo-orchitis. On examination, the majority showed enlarged prostate but only 20% present with the classic signs of prostatic fluctuance and tenderness on DRE (Sohlberg et al., 1991). Abscess can be identified as irregular hypoechoic area containing diffuse mid-range echoes within an enlarged gland (Fig. 8 C). Once identified, the lesions may be aspirated transperineally under ultrasound control (Doble & Carter, 1989).

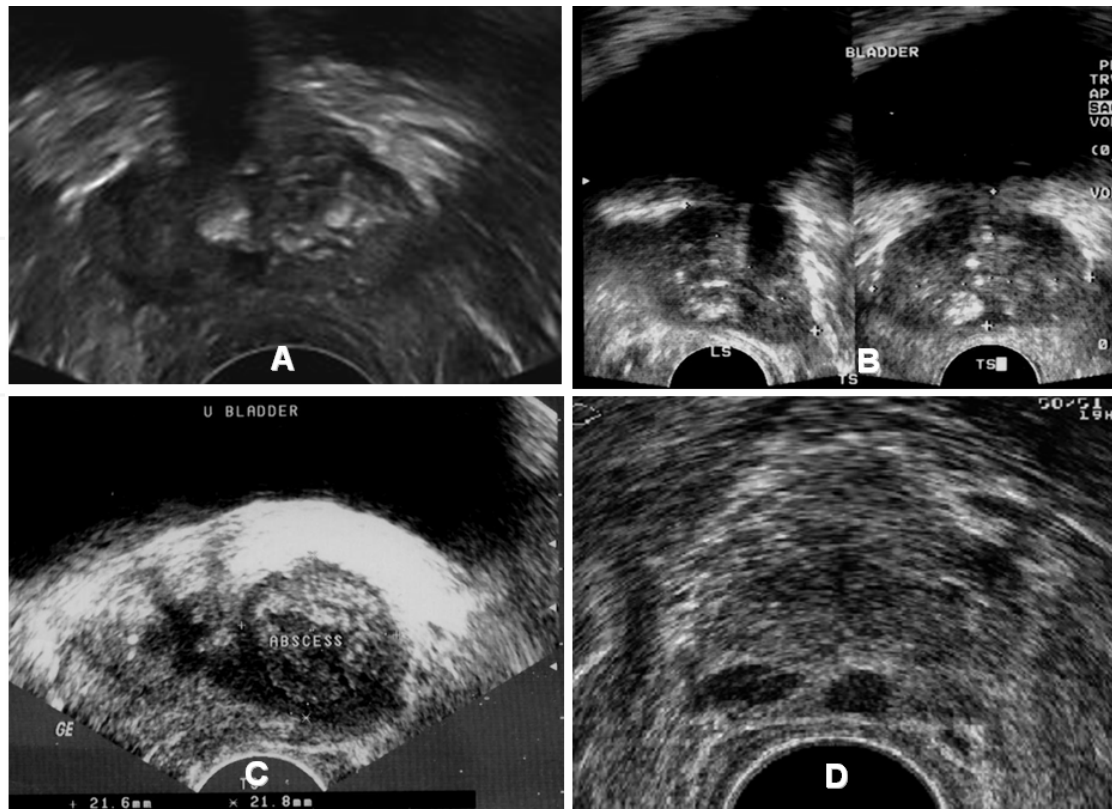


Fig. 8. (A) TRUS of a patient with chronic prostatitis shows calcification of periurethral tissue. (B) TRUS of another patient with chronic prostatitis shows calcification of peripheral zone. (C) TRUS of a case of prostatic abscess with a relatively thick wall and echogenic fluid content. (D) TRUS of a patient with granulomatous prostatitis shows multifocal hypoechoic lesions in the peripheral zone mimicking prostatic cancer

The exact aetiology of granulomatous prostatitis remains undetermined. It is thought to be due to ductal obstruction and ectasia with subsequently extravasation of luminal contents into the glandular stroma. In most patients, these changes are thought to be idiopathic but in others, it can be also linked with specific infecting agents (tuberculosis, schistosomiasis, and fungi). In patients with granulomatous prostatitis, the prostate is usually firm, nodular or indurated on DRE, PSA may be elevated. Patients may present with symptoms of outflow tract obstruction, acute retention or urinary infection. Sonographic findings are single or multiple areas of low echogenicity in the peripheral zone (Fig. 8D) or heterogeneous echotexture of the gland. The hypoechoic areas are indistinguishable from carcinoma and diagnosis must be established by biopsy (Clements et al., 1993).

5.3 Prostatic calcifications and calculi

Primary prostatic calculi develop in the prostatic ducts and acini. They are usually multiple and small (1-5mm). Secondary dystrophic calcifications are associated with infection, obstruction, necrosis in a prostatic adenoma or radiation therapy. They are usually larger and more irregular than primary calculi. It needs to be emphasized that dystrophic prostatic calculi are not precancerous (Hricak, 1990). Sonographically calcifications appear as bright echogenic foci with or without posterior acoustic shadowing. Calculi can be seen within the seminal vesicles, vassal ampulae or ejaculatory ducts (Fig. 9).

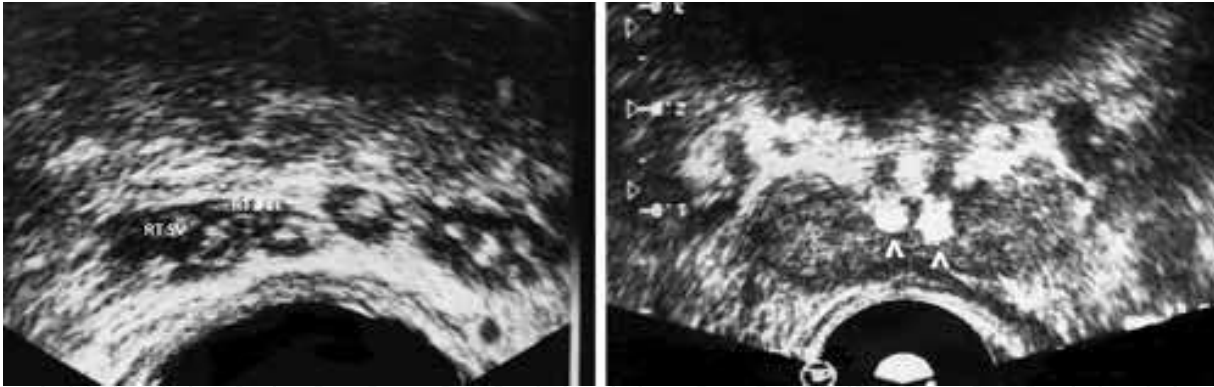


Fig. 9. (A) TRUS shows multiple flecks of calcifications seen in both seminal vesicles (SV) and vassal ampulae. (B) TRUS shows bilateral ejaculatory ducts calculi (arrow heads) in a patient with obstructive azospermia

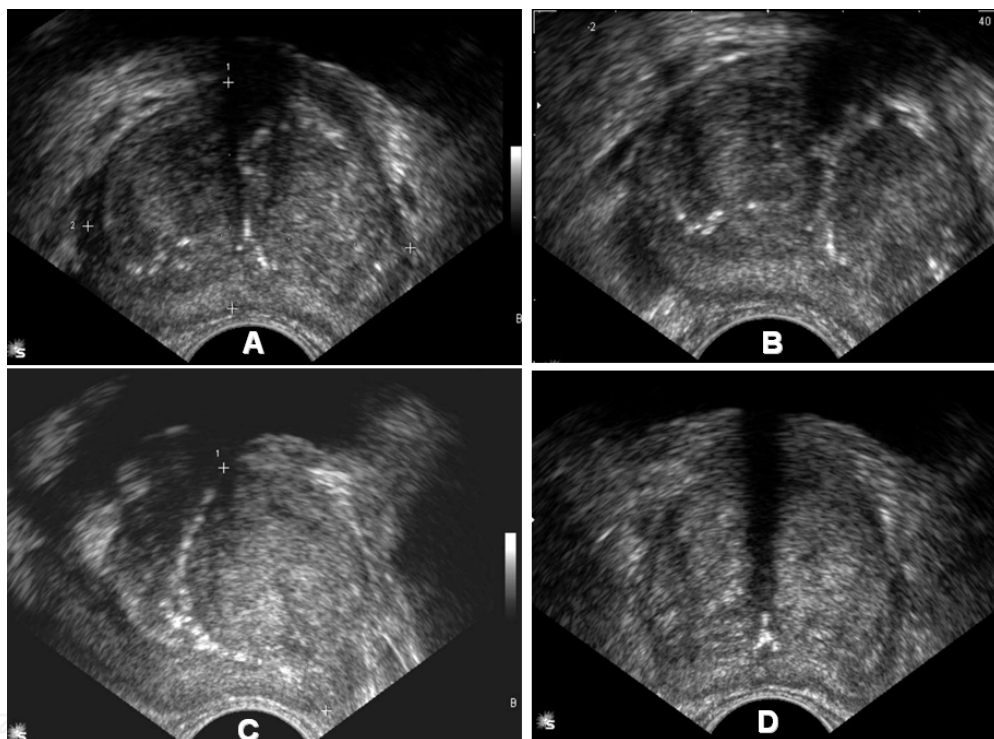


Fig. 10. (A) & (B) TRUS of BPH shows bilobed adenoma causing compression and flattening of the PZ. (C) TRUS of another case of BPH shows calcified surgical capsule separating the adenoma from the PZ. (D) TRUS of another patient with BPH shows large bilobed adenoma separating from the flattened PZ by hypoechoic surgical capsule

5.4 Benign prostatic hyperplasia

Benign prostatic hyperplasia (BPH) is rarely seen in males less than 40 years of age. It affects 50 to 70% of men older than 60, and 80 to 85% of men older than 80 years. BPH begins in the inner region of the prostate adjacent to the urethra. BPH may be diffuse or focal; forming prostatic adenoma. The normal prostatic tissue is displayed caudally and posteriorly to form the surgical capsule (Mc Neal, 1983). Ultrasound is the primary imaging modality for evaluation of the aging men with known or suspected BPH. By transabdominal US prostatic

size, weight, shape and intravesical extent can be determined. Uncomplicated BPH usually produce a diffusely – altered inhomogenous echotexture, but distinct nodular enlargement cannot be differentiated from the surrounding gland (Fig. 5). Residual urine and bladder volume can be measured by the same formula used for estimating prostatic size (volume=0.52 x d1 x d2 X d3. Upper tract changes secondary to BPH are best evaluated using abdominal US. TRUS provides the best cross-sectional anatomy of the prostate and it is more accurate than transabdominal US to assess volume of the prostate and adenoma. BPH has a varied echotexture but is usually homogenous solitary or multiple adenomas (hyperplastic nodules) may be imaged, confined or extending outwards from the central gland often compressing the peripheral zone (Fig. 10). Although symmetry is the rule asymmetrical increase in size, especially near the bladder neck are common. Cysts, calcifications, prostatitis, infarctions and carcinoma may be coincident with BPH. The thick surgical capsule interposed between the central and peripheral gland can be appreciated. (Naryan & Foster, 1991).

5.5 Prostatic cancer

Carcinoma of the prostate is the most common human cancer, found at autopsy in 30% of men at age 50, 60% of men at age 80 – 90 up to 100% in those over age 90. It is now the second most common cancer in men. Pathological evidence of prostate cancer is found in 10-20% of patients undergoing surgery for BPH. 68% of prostatic carcinomas originate in the PZ, 24% in the TZ, and 8% in the CZ. Carcinoma of the prostate is often adenocarcinoma with varying grades of differentiation in 95% (Mc Neal, 1983). Unlike lung and colon cancer, prostatic cancer is predominantly latent. The patient may present with the symptoms and signs of prostatism and occasionally haematuria. It has been speculated that prostatic cancer disseminates first by invading into the periprostatic tissues, then by lymphatic embolization, and finally by hematogenous dissemination. Prostatic cancer can also spread by direct local invasion and through vascular and lymphatic channels. Seminal vesicle invasion almost always results from direct spread of the tumor into the ejaculatory duct while crossing inside and prostate. The primary field of lymphatic drainage of the prostate includes the perivesical, hypogastric, obturator, presacral and preceliac lymph nodes. The obturator nodes are the commonest site of involvement (Mc Laughlin et al., 1976). Osseous metastases are present in about 85 percent of patients dying of prostatic cancer. Osseous metastases involve the cancellous bone, altering the normal internal architecture with proliferating osteoblasts and new bone formation. The commonest sites for visceral metastases from prostatic cancer lung, liver and adrenal gland, but virtually any organ may be involved. Pulmonary metastases, occurring in 25 to 38 percent of patients dying of prostatic cancer. Metastases to the central nervous system usually occur in the meninges and may be clinically silent. Other neurogenic manifestations of prostatic cancer include organic brain syndrome, radiculopathy, and paraneoplastic syndromes (Jacobs, 1983).

5.5.1 Detection of prostate cancer

TRUS is useful for early detection of prostate cancer, guided biopsy, local staging, and follow up after treatment. Its role in screening of asymptomatic men is still controversial. (Clements et al., 1993). The first step in any sonographic examination of the prostate should be to gain an overall impression of the gland's shape and size. An irregular asymmetric

gland often signals malignancy even in the absence of the identifiable lesion. Even small prostatic cancer often alters the shape of the prostate. Distortion or bulging of the posterior boundary of the prostate is suggestive of the presence of cancer. Lateral distortion is of less significance because hyperplastic nodules of the TZ cause considerable asymmetric bulging. In advanced cancer, discontinuity of the capsule or seminal vesicles irregularity often can be seen (Shinohara et al., 1989).

Prostate cancer has different echotexture; it may be hypoechoic, isoechpic or hyperechoic (Fig. 11). Most cancers consist of a dense mass of cells which destroys the normal glandular structure. The malignant tissue contains few sonographically detectable interfaces and therefore appears hyperechoic region in relation to the adjacent normal tissue. The most common feature of all visible cancer is a central hypoechoic region relative to the peripheral zone of the normal prostate. The margins of the tumor are ill defined as the malignant cells invade between normal prostatic acini (Shinohara et al., 1989). The hypoechoic tumors represent 70-75% of prostate tumors (Hamper & Sheth, 1993). Approximately 30-35% of clinically detected prostate cancer cannot be distinguished from the normal surrounding prostatic tissue and is termed isoechoic. Several features may contribute to cancer being undetectable by US: tumor size, grade, location, and stage, technique of the study, equipment used and the experience of the operator. Absence of the normal margin between the PZ and TZ in a rounded prostate should alert the sonographer to the possibility of a large infiltrating tumor. Also, a palpable abnormality in the presence of an apparently normal US scan should be biopsied to avoid missing an isoechoic cancer (Shabsigh et al., 1989). In case of presence of large adenoma of BPH, the PZ is compressed. So, it is less easy to detect a PZ cancer (Shinohara et al., 1989). Hyperechoic tumors are rare. Prostatic calculi that have been engulfed by cancer may account for a mixed echogenic pattern. Hyperechoic foci within the tumor correspond pathologically to comedonecrosis and calcification within highly undifferentiated anaplastic tumors or unusual deposits of intraluminal crystalloid secretions.

The sonographic appearance of early prostate cancer is not specific. The positive predictive value for a hypoechoic focal lesion to be cancer has ranged from 0% to 50%. Overall, the incidence of malignancy in US suspicious lesion is 20% to 25% (Hamper & Sheth, 1993). Information from US-guided biopsy of the prostate has shown that many suspicious areas seen on TRUS do not correspond to cancer: negative biopsy rates of 58 to 70.8% have been reported (Shabsigh et al., 1989). There is a big list of differential diagnosis of intraprostatic hypoechoic lesions. First anatomic structures as periurethral tissue, ejaculatory duct complex, periprostatic veins and neurovascular bundles. Second are benign prostatic diseases as hyperplastic nodule (stromal types), prostatitis, abscess, cysts and hematoma. Lastly sonographic artifacts as inappropriate use of the focal range of transducer, acoustic shadowing, reverberation artifacts and edge effect (Shinhara et al., 1989). Mc Neal and associates have emphasized the importance of measurement of the volume of prostate cancer as a determinant of pathologic stage and prognosis. They described a strong association between tumor volume and the incidence of extracapsular extension and lymph node metastases (Mc Neal et al., 1986). Estimation of tumor volume by TRUS is often inaccurate for two reasons. Tumor size is usually underestimated, as the tumor tends to infiltrate and invade between normal prostatic tissues. So, the margin of the tumor may therefore be indistinguishable from normal prostate. Second is prostate cancer is often

multifocal. So, U.S underestimates the maximum diameter of a focus of cancer by an average of 4.2 mm (Shinohara et al., 1989).

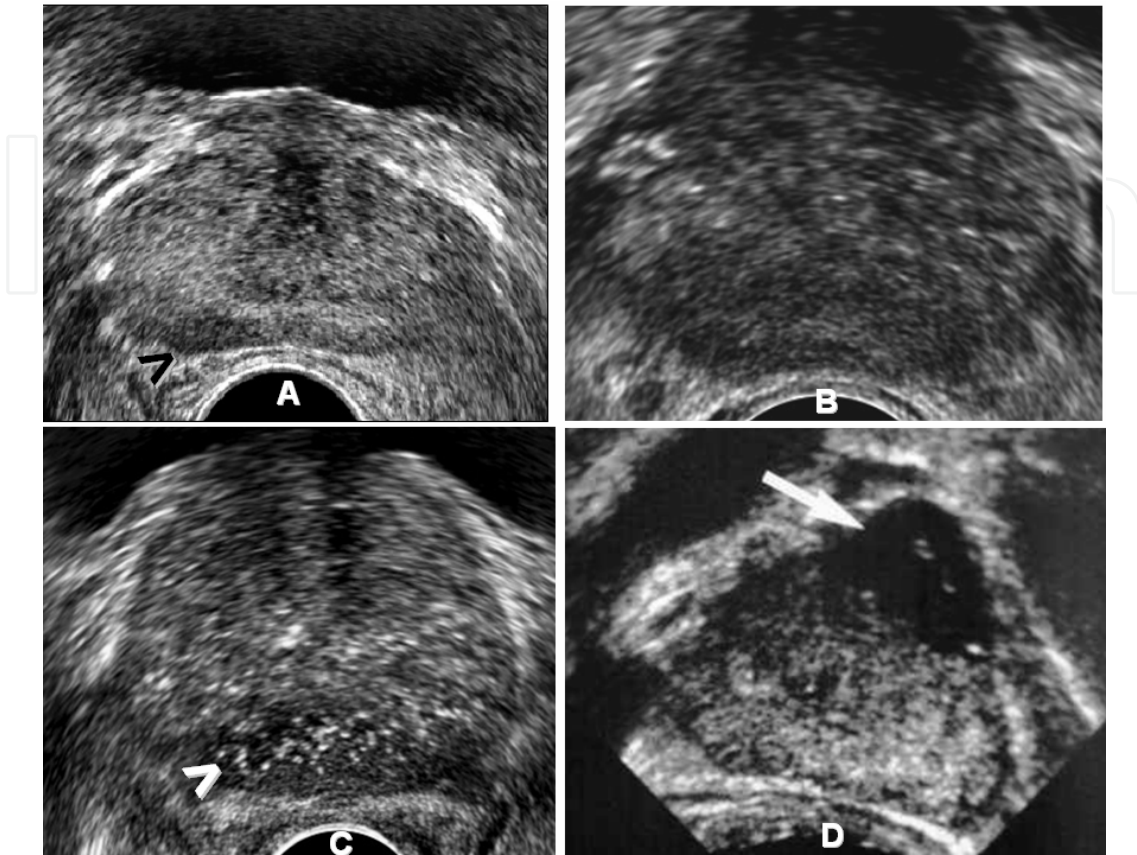


Fig. 11. TRUS of four different patients with prostate cancer. The carcinoma appears as focal hypoechoic area (arrow head) in the right PZ (A), diffuse hypoechoogenicity of the whole gland (B), focal hyperechoic area (arrow head) in the posterior PZ (C) and focal hypoechoic area (arrow) in the central gland (D)

5.5.2 Extra capsular extension of prostate cancer

Prostate cancer spreads locally through pathways of least resistance. The areas of local spread include the invaginated extraprostatic area around the ejaculatory duct to the seminal vesicles, at the apex where the capsule is deficient, areas of capsule penetration by superior and inferior neurovascular bundles. The prostatic capsule usually cannot be distinguished sonographically from the prostatic parenchyma. Consequently, the continuous hyperechoic border around the normal prostate, (usually referred as the “capsule”), is actually represents the acoustic interface between the prostate and the periprostatic fat (Scardino et al., 1989). Sonographic signs of capsular penetration include bulge or irregularity of the prostate contour and disruption or discontinuity of the echogenic periprostatic boundary echo (Hamper & Sheth, 1993). Spread of the cancer to the neurovascular bundle is suspected if the tumor is close to the posterolateral aspect of the prostate with irregularity of the contour at this region as well as interruption of the echogenic periprostatic boundary echo. TRUS is able to detect neurovascular involvement with sensitivity of 66% and specificity of 78% (Fig. 12 and 13).

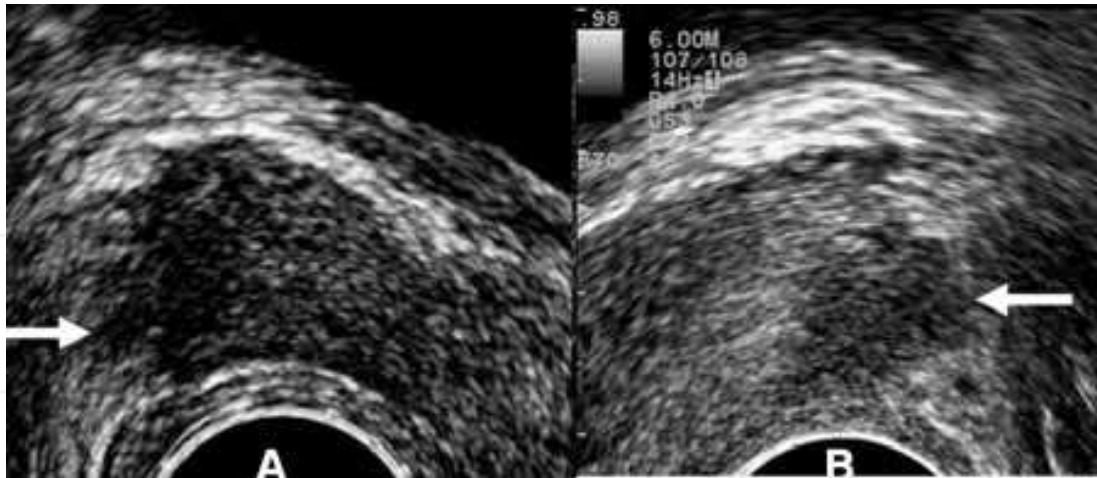


Fig. 12. Two different patients with right and left lateral extracapsular extension (arrows)

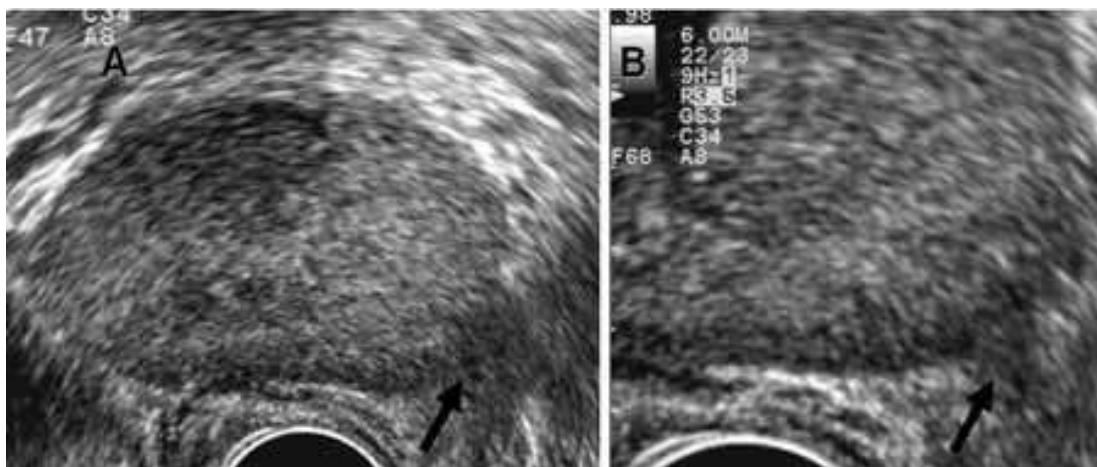


Fig. 13. A case of prostate cancer with left posterolateral extension through the neurovascular bundle (arrows)

The pattern and extent of seminal vesicle invasion vary widely. Type I is the most common pattern. It shows invasion along the ejaculatory ducts into the seminal vesicle. Type II is the second most common pattern. The invasion of seminal vesicle occurs from a tumor that penetrates the capsule and invades the seminal vesicles in continuity. Type III is the least common pattern, where small isolated foci of tumor in the seminal vesicles. The sonographic criteria for seminal vesicles invasion have traditionally been described as asymmetry in size, irregularity in outline, atrophy and distension, but the validity of these signs has rarely been substantiated by surgical or pathological staging (Shinohara et al., 1988). The accuracy of detection seminal vesicle invasion using sonography is 86% (Terries et al., 1990). The apex of the prostate must be carefully assessed sonographically to detect involvement of the rhomboid area. This area bounded by the prostate proximally, the rectourethralis muscle distally, the membranous urethra anteriorly and the rectum posteriorly. It is best demonstrated by TRUS on the sagittal view. TRUS has no role in nodal staging. Also, it had limited role in detection of invasion of neighboring tissue, e.g. bladder, rectum and muscles of the pelvic side wall. These disadvantages of TRUS can be explained by its limited field of view (Scardino et al., 1989).

5.5.3 Response to treatment of prostate cancer

After treatment by orchiectomy and hormonal therapy, the gland becomes smaller and assumes a more circular shape. Most of the decrease in volume occurred within the first three months. A variable series of changes in the US appearance of the gland may be seen. In some patients, the area of abnormal echogenicity may persist. In others, it disappears. The integrity of the capsule may appear to be restored in patients with previous capsule breach. It may be extremely difficult to demonstrate US whether the active cancer is still present or not (Clements et al., 1989). Following radiotherapy for cancer, the prostate becomes small and echogenic. Anechoic or hypoechoic lesions following radiotherapy frequently represent persistent cancer and the positive predictive value of such lesions for cancer is 91%. Most foci of cancer with marked radiation effect tend to be isoechoic. The non malignant prostate tissue generally retains its normal echogenic appearance after irradiation. Lesions over 5mm in the diameter persisting for 12 months following radiotherapy are suspicious of malignancy and should be biopsied (Egawa et al., 1991). A decrease in total prostate volume is not a reliable indicator of prognosis as normal and malignant prostatic tissue will shrink in response to radiotherapy. Measuring PSA is probably more useful in the follow up of the prostate cancer (Richards, 1992). After radical retropubic prostatectomy (for clinically non invasive prostatic cancer), the patients are routinely followed up at periodic interval with DRE and measuring PSA. Elevation of PSA above the female range indicates either local progression, recurrence of distant metastases. Post-operative mature fibrotic tissue at the site of operation is difficult to distinguish from recurrent tumors by means of TRUS. The main value of TRUS in case of presence of post operative palpable mass may be in accurate positioning of the biopsy needle about the vesico-urethral anastomosis (Wasserman et al., 1992).

6. Ultrasound guided prostatic biopsy

The most important role for TRUS is to provide visual guidance for biopsy. Approximately 25% to 30% of cancers are isoechoic, random biopsies of the PZ, in addition to sampling all suspicious lesions should be done. In the technique of random prostatic biopsies, multiple samples are taken from different parts of the gland mainly apex, mid gland and base bilaterally (Hamper & Sheth 1993). In general, TRUS guided prostate needle biopsy should be performed in men with an abnormal DRE, an elevated PSA (>4.0 ng/ ml) or PSA velocity (rate of PSA change) >0.4 to 0.75ng/ ml/ yr. Also, men who were diagnosed with high-grade prostatic intraepithelial neoplasia (PIN) or atypia on a previous prostate needle biopsy should undergo a repeat biopsy 3 to 12 months later. Less commonly agreed upon recommendations for TRUS guided prostate needle biopsy include, age-specific PSA elevation, low percentage free PSA (< 22% to 25%), and prostate specific antigen density (PSAD) > 0.15, which is a measure of the amount of PSA relative to the overall prostatic volume (Hamper & Sheth 1993). US-guided prostate biopsies can be performed either transperineally or transrectally.

Transperineal approach is the first way described for US-guided prostate biopsy in 1981. The probe is fixed to a stabilizing biopsy stand. The perineum should be infiltrated with local anesthetic. The entire gland is inspected and once a suspected area is identified, the biopsy needle is inserted and the track of the needle is monitored on the viewing screen. When the

needle tip approaches the area to be biopsied, the needle is positioned so that the cutting section can be passed through the abnormal area under visual guidance (Muldoon & Resnick, 1989). The drawbacks of transperineal U.S guided biopsy are difficult needle due to relatively long transperineal needle path, it is time consuming procedure, and patients tolerate the procedure poorly because of perineal pain and side effects of local anaesthesia. (Clements et al., 1993). Transperineal approach is preferable if prostate abscess or inflammatory disease is suspected.

Transrectal approach was first described in 1987, since then, this technique has been described as a superior method of performing a core biopsy of the prostate (Weaver et al., 1991). The transrectal approach offers the advantage of a shorter needle with easier needle placement, and quicker and relatively painless procedure. Local anesthesia is not required and it is done on an out-patients basis (Clements et al., 1993). Hodge et al reported that systematic sampling of the prostate guided by TRUS improved the detection rate of prostate cancer over merely sampling hypoechoic or other lesions. By taking sextant biopsies from the mid lobe (parasagittal) of each side of the prostate at the apex, middle, and base (Fig. 14), the cancer detection rate was superior to lesion-directed biopsies (Hodge et al., 1989). This technique was accepted over the time as the standard of care and helped to emphasize that TRUS was more useful for biopsy than for imaging. In the current PSA era, though, most men who are undergoing prostate biopsy do not have palpable abnormalities or hypoechoic lesions. This has led investigators to question the sampling adequacy of the standard sextant prostate biopsy template and to propose alternate "extended pattern" biopsy schemes to improve prostate cancer detection. The alternate prostate biopsy templates aim to improve sampling of the prostate by either increasing the number of core biopsies taken and/ or by directing the biopsies more laterally to better sample the anterior horn (Chen et al, 1999, Naughton et al., 2000). During biopsy, the puncture path is shown on the monitor as electric dotted line. The probe should be positioned so that the puncture path passes through the designated area. Without moving the probe, the needle is introduced through the needle guide and the needle tip is positioned proximal to the suspicious area. A trigger action biopsy gun is used to obtain a core specimen in an instance once the biopsy needle is in place. The biopsies performed while the biopsy needle is directed parallel to the transducer in the sagittal plane so the needle seen as an echogenic linear structure approaching the suspicious area, instead of an echogenic dot in the axial plane (Lee et al., 1988).

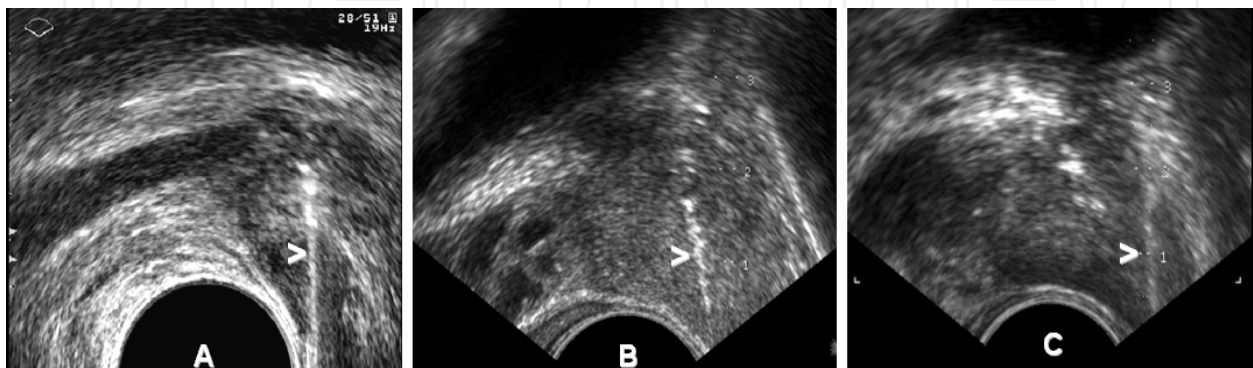


Fig. 14. Systematic TRUS-guided biopsy of the upper (A), middle (B) and lower (C) parts of the lateral regions peripheral zone (arrowheads)

7. Role of new ultrasound techniques in diagnosis of prostate cancer

Conventional gray-scale US has low sensitivity and specificity and is mainly used for guiding systematic prostate biopsies. With the development of new US techniques, such as three dimensional US color and power Doppler US, the use of US contrast agents and elastography, the role of US for prostate cancer detection has dramatically improved.

7.1 Three dimensional (3D) US of the prostate

It gives views of the prostate in the 3 orthogonal planes; sagittal, transverse and coronal and in any other oblique planes (Fig. 15). The detection rates of prostate cancer were significantly improved with 3D- TRUS. Also it may improve the biopsy yield by determining appropriate sites for target and systematic biopsies (Cool et al., 2008, Shen et al., 2008). With 3D imaging, spatial relationships much clearer, so radiologist/ urologist can better assess the extent of disease. It may make it easier to determine whether the “prostate capsule” has been penetrated to detect possible extra-capsular tumor extension which is a key factor in staging of prostate cancer. It provides valuable information to plan for alternative therapies, like radiotherapy of the prostate and robotic prostatectomy. The 3D images are saved and they can be reviewed as many times as needed. Diagnosis can be achieved by retrieving the saved images which is most convenient for the operator and patient, leading to faster patient turnaround (Liang et al., 2010, Bax et al., 2008).

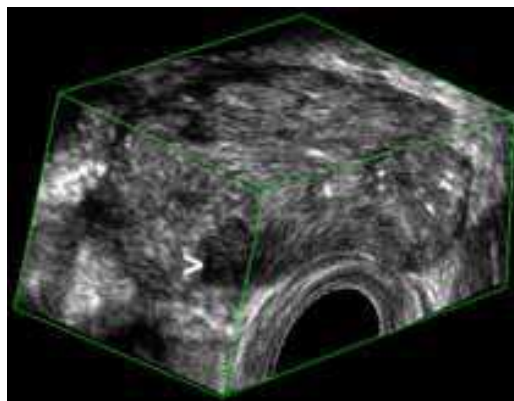


Fig. 15. 3D images of a prostate with cancer. The image has been ‘sliced’ to reveal a hypoechoic lesion in the right side of the PZ (arrowhead) proved to be a cancer

7.2 Color Doppler sonography of the prostate

Color Doppler TRUS (CD-TRUS) has been applied to evaluate the vascularity within the prostate and the surrounding structures. Preliminary studies demonstrated increased flow within or surrounding prostate neoplasm, whereas prostatitis and BPH showed a diffusely abnormal flow. However, the flow of focal prostatitis was not significantly different from cancer. By using objective measures, as resistive indices, no statistically significant difference was found between cancer and benign conditions (Rifkin et al, 1993). CD-TRUS may help in determining the site of biopsy. If the level of PSA is elevated with DRE normal in one patient, the presence of hypervascular focal lesion in PZ makes the lesion the target of the biopsy. But, if the nodule is hypovascular, we have to biopsy the anterior part of the gland to detect carcinoma of the TZ. (Cornud et al., 1993). Early results have suggested that up to 85% of men with prostate cancers greater than 5 mm in size have visibly increased

flow in the area of tumor involvement. In addition, hypervascularity may be seen in patients with more difficult to identify, isoechoic and hyperechoic lesions (Fig. 16). Unfortunately, subsequent studies suggested that some prostate cancers are hypovascular. Many studies prove the benefits of CD-TRUS for the evaluation of prostatic disease, especially carcinoma. The motivation behind the application of color Doppler US is to detect tumor neovascularity. Cancerous tissue generally grows more rapidly than normal tissue and demonstrates increased blood flow; as compared to normal tissue and benign lesions. Color Doppler US may demonstrate an increased number of visualized vessels, as well as an increase in flow rate, size and irregularity of vessels within prostate cancer (Newman et al., 1995 Littrup et al., 1995, Ismail et al., 1997)

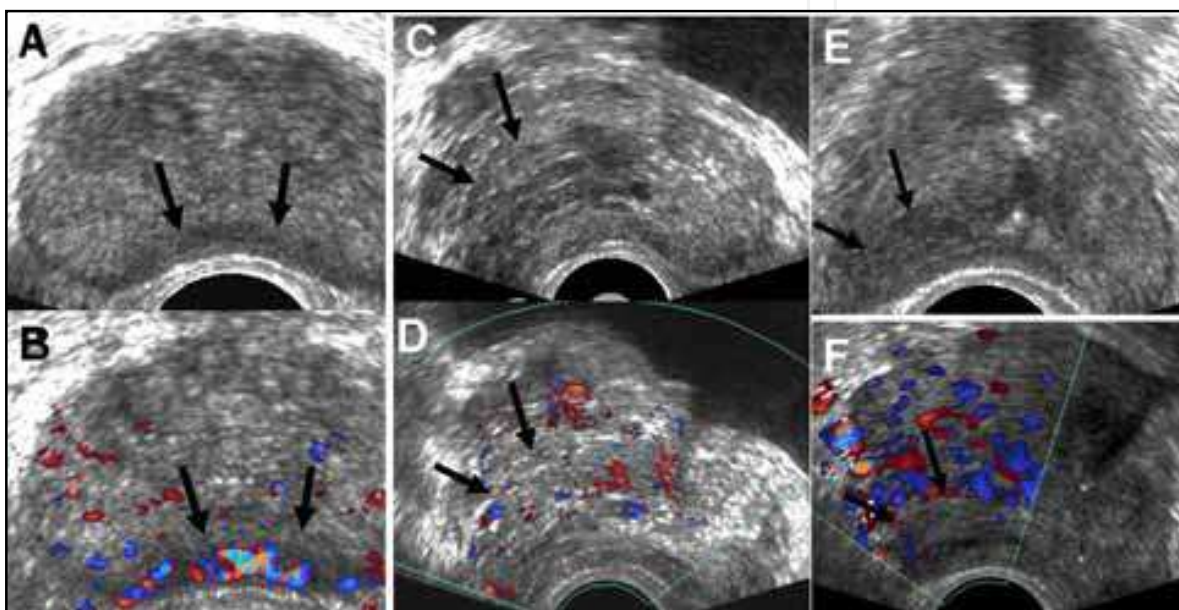


Fig. 16. (A) TRUS shows hypoechoic areas proved to be cancer (arrows). (B) Color-Doppler shows the same area to be of high vascularity (arrows). (C) TRUS of another patient with prostate cancer appears as hypoechoic area (arrows). (D) The same area appears with normal vascularity in color Doppler. (E) TRUS of a third patient with hypoechoic lesion of prostate cancer appears as hypoechoic (arrows). (F) The same lesion appears of low vascularity in color Doppler

7.3 Power Doppler sonography of the prostate

Power Doppler US is an amplitude-based technique for the detection of flow. It is more sensitive to slow flow and is less angle-dependent than color Doppler US. This technique has been less commonly applied to the assessment of prostate tumor vascularity, and there are few papers addressing its use. Some studies showed that prostate cancer are hypervascular by power Doppler (Fig. 17) so it may be useful in detection of prostate cancer (Inahara et al., 2004). Halpern et al assessed the value of gray-scale, color and power Doppler US for detection of prostatic cancer. They investigated 251 patients prior to biopsy and they concluded that power Doppler may be useful for targeted biopsies when the number of biopsy passes must be limited but that there is no substantial advantage of power Doppler over color Doppler (Halpern et al., 2000).

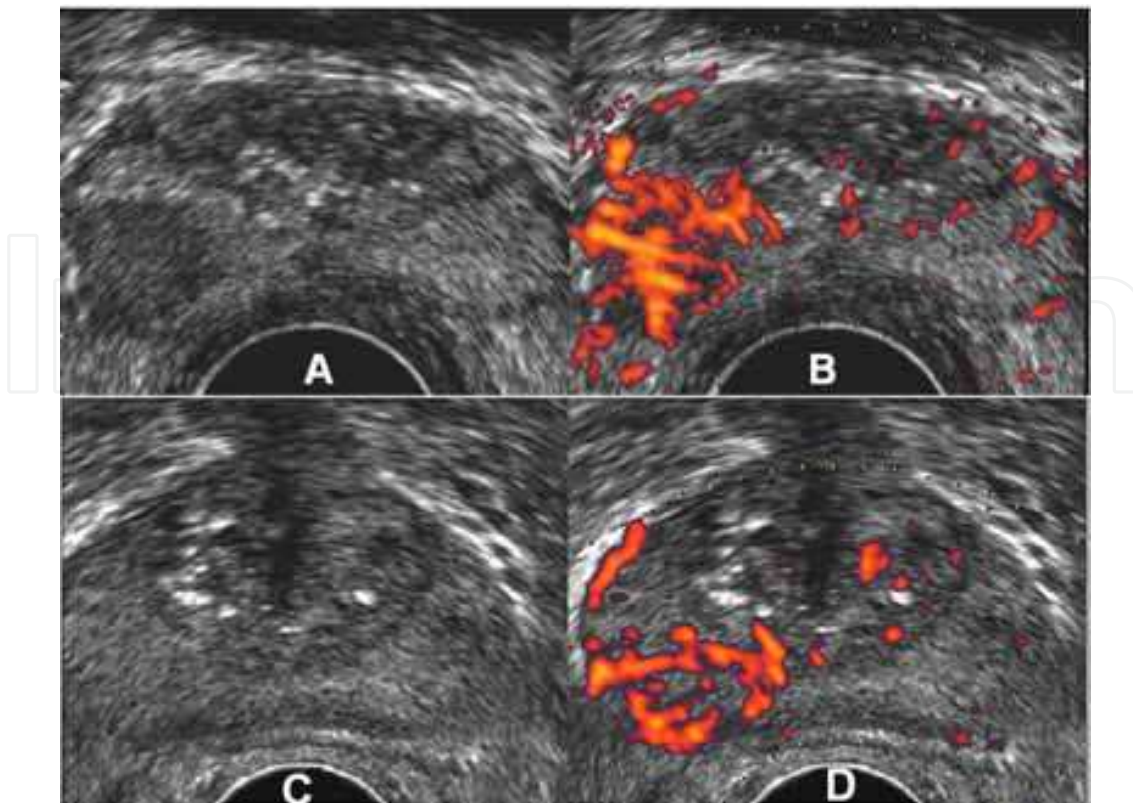


Fig. 17. (A) TRUS show a hypoechoic lesion in the right posterolateral aspect of the peripheral zone proved to be cancer. (B) The same area is hypervascular in power Doppler (C) TRUS in another patient with prostate cancer shows no evident focal lesion in grey scale US. (D) Power Doppler of the same patient show focal area of increased vascularity in the right side of the peripheral zone proved to be carcinoma by targeted biopsy

7.4 Contrast enhanced ultrasound imaging

Recently developed US contrast agents can improve the detection of low-volume blood flow by increasing the signal-to-noise ratio. Unlike radiographic contrast media, which diffuse into the tissue and may obscure smaller vessels, microbubble echo-enhancing agents are confined to the vascular lumen, where they persist until they dissolve. They have two important acoustic properties, first, they are many times more reflective than blood, thus improving flow detection. Second, their vibrations generate higher harmonics to a much greater degree than surrounding tissues (Forsberg et al, 1998). Bree RL and De Dreu SE showed that contrast enhanced color Doppler US had a sensitivity of 53%, specificity of 72%, and a positive predictive value of 70% in distinguishing prostate cancer from benign lesions in 72 patients identified by PSA screening (Bree RL & DeDreeu SE,1998). Most investigators showed increased sensitivity in detection of prostate cancer after the use of contrast enhanced US (Fig. 20). In the study of Bogers et al, they showed that sensitivity of enhanced images was 85% (specificity 80%) compared with 38% for unenhanced images (specificity 80%) and 77% for conventional gray-scale transrectal US (specificity 60%) (Bogers et al., 1999). Frauscher et al reported the value of contrast enhanced color Doppler in a prospective study in 90, and 230 male screening volunteers (Frauscher et al., 2001, 2002). They found that targeted biopsies based on contrast enhanced color Doppler detected as many cancers as

systematic biopsies, with fewer than half the number of biopsy cores. Halpern et al, in their prospective study of contrast-enhanced transrectal US in 60 patients who underwent sextant biopsy of the prostate concluded that the sensitivity increased from 38% at baseline to 65% after contrast injection (Fig. 18). However there was no significant change of specificity between baseline study (83%) and during contrast aging (80%) in the same study (Halpern et al., 2001).

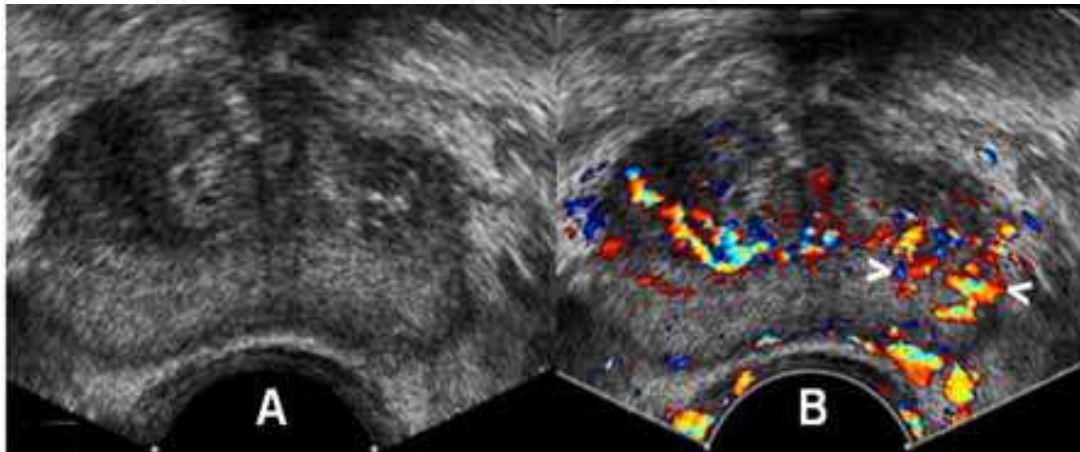


Fig. 18. (A) TRUS of a patient with prostate cancer show no evident focal lesions in grey scale US. (B) Contrast enhanced TRUS shows focal area of hypervascularity in the left side of the peripheral zone (arrowheads) proved to be carcinoma by targeted biopsy

7.5 Elastography of the prostate

Elastography or strain imaging was first described in 1991 (Ophir et al., 1991). This technique can be used to detect degree of stiffness of the tissues. In a pilot study done by Klauser et al, patients with clinically localized prostate cancer who underwent radical prostatectomy were examined prospectively. They found that elastography detected 28 of 32 cancer foci (sensitivity 88%) and they concluded that elastography is a sensitive new imaging modality for the detection of prostate cancer (Klauser et al., 2003). Konig et al. evaluated elastography for biopsy guidance for prostate cancer detection in 404 men underwent systematic sextant biopsy. They found that in 127 of the cancer proved 151 cases (84.1%), prostate cancer was detected using elastography as an additional diagnostic feature. They concluded that it is possible to detect prostate cancer with a high degree of sensitivity using real-time elastography in conjunction with conventional diagnostic methods for guided prostate biopsies (Konig et al., 2005). Supersonic shear imaging (SSI) is a new US-based technique for real-time visualization of soft tissue elastographic properties. Using ultrasonic focused beams, it is possible to remotely generate mechanical vibration sources radiating low-frequency, shear waves inside tissues (Bercoff et al., 2004). Athanasiou et al studied quantitative ultrasonographic elastography of breast lesions in 46 women. They concluded that SSI provides quantitative elasticity measurements, thus adding complementary information that potentially could help in breast lesion characterization with B-mode US (Athanasiou et al., 2010). Recently a preliminary study by Correias et al done to evaluated the feasibility of TRUS quantitative Shear Wave Elastography (SWE) for prostate cancer evaluation in 21 patients presenting with increased PSA values (Fig. 19). Elasticity measurements and ratios between nodules and adjacent parenchyma were

calculated. They found that signals were obtained in both the peripheral and the transition zones with good correlation to anatomical areas, macro-calcifications exhibited very high stiffness values and prostate cancer nodules exhibited a high stiffness than the adjacent peripheral gland. Also they noticed that peripheral adenomatous hyperplasia and focal prostatitis exhibited a significantly lower stiffness. They concluded that TRUS quantitative SWE is a feasible technique for prostate cancer evaluation. It provides additional information about stiffness of nodules localized in the peripheral zone (Correas et al., 2011). These preliminary results are encouraging but a larger multicentric evaluation remains necessary.

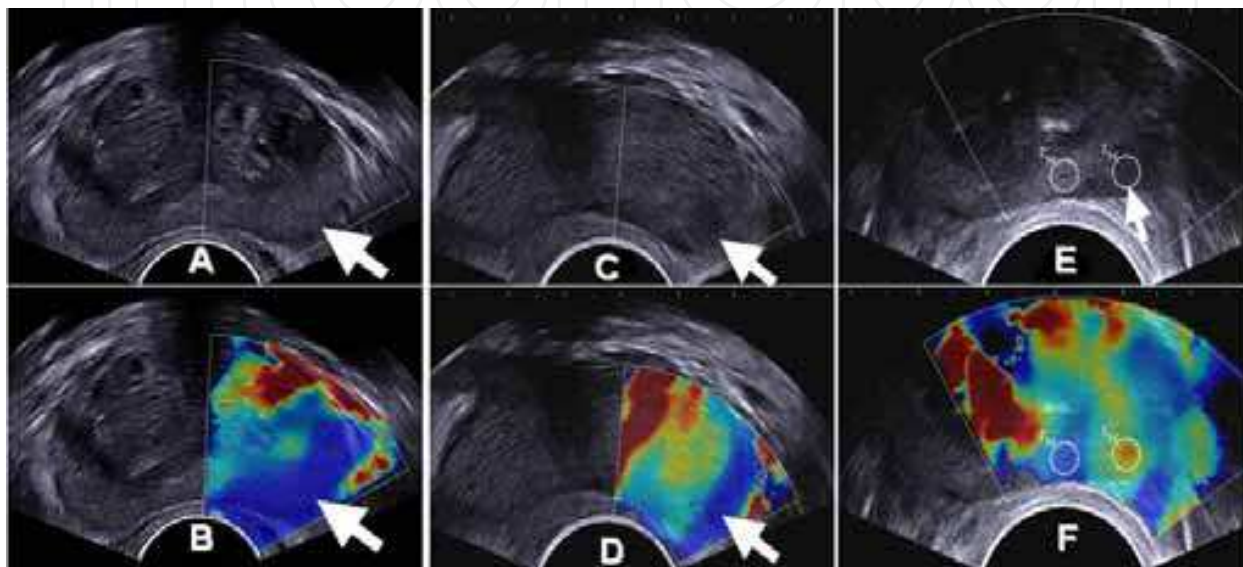


Fig. 19. (A) TRUS of a normal homogeneous PZ. (B) TRUS-SWE shows homogeneous blue coding of PZ (arrow) indicating its soft texture. (C) TRUS of another patient shows a hypoechoic area in left PZ proved to be carcinoma (atypical pattern). (D) TRUS-SWE of the same patient shows the focal area has blue coding (arrow) indicating its soft texture. (E) TRUS of another patient with a hypoechoic nodule in the left PZ proved to be carcinoma (arrow). (F) TRUS-SWE of the same patient shows a strong increase in stiffness values of the focal area (red) with a ratio of 2.8 compared to the surrounding PZ (typical pattern) (adapted from Correas et al 2011)

8. Role of ultrasound in prostate cancer treatment

Recent interest in focal therapy for localized prostate cancer has been driven by downward stage migration, improved biopsy and imaging techniques. Several techniques have potential for focal ablation of prostate cancer.

8.1 TRUS-guided cryotherapy for prostate cancer

Cryotherapy is tissue ablation by local induction of extremely cold temperatures. The first use cryoablation in urological disorders started in the 1960s for management of benign prostatic hyperplastic tissue (Gonder et al., 1966). This was followed shortly thereafter by the treatment of prostate cancer via an open perineal approach (Fig. 20). The major impediment to early acceptance of the modality, however, was the inability to accurately

monitor cryoprobe placement and ice-ball formation. Major advances in the past 20 years, which have reinvigorated investigation into the use of cryotherapy for prostate cancer, have included the use of TRUS monitoring of probe placement and freezing (Onil et al,1993). A significant recent development was the introduction of cryotherapy probes that use argon gas rather than liquid nitrogen (De La Taille et al., 2000). Outcomes have now been reported as late as 7 years following treatment of prostate cancer and seem to compare favorably with contemporary series of patients who receive radiation therapy (Bahn et al., 2002). Marberger et al reported that cryotherapy has been used for some time as a form of first-line therapy for complete ablation of the prostate or and as a second-line therapy for local recurrence after radiotherapy (Marberger et al., 2008).

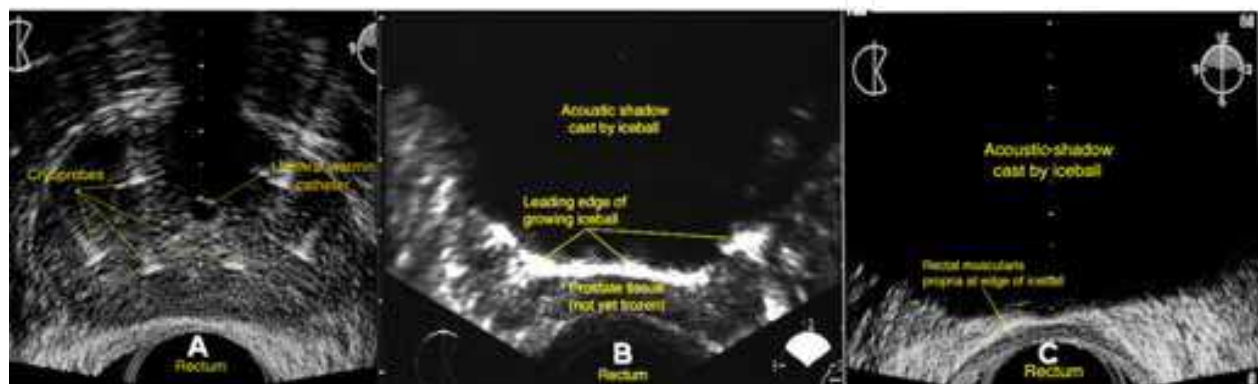


Fig. 20. (A) TRUS of the prostate illustrating placement of the cryoprobes and urethral-warming catheter. (B) TRUS of the prostate during cryoablation showing the ice ball, growing posteriorly, is echodense and casts a dark acoustic shadow. (C) The ice ball extends posteriorly to include the whole prostate tissue. Transrectal sonogram of the prostate illustrating placement of the cryoprobes and urethral-warming catheter

8.2 High-intensity focused ultrasound (HIFU)

HIFU is one of the newer methods that have been developed to treat early stage prostate cancers. High energy is delivered to the affected area by ultrasound, this result in the targeted cancerous cells heating up and being destroyed. Using extracorporeal HIFU, temperatures of greater than 60°C can be achieved in the target tissue. The prostate can be easily treated with this modality via a transrectal probe. Gelet et al pioneered the use of transrectal HIFU in the treatment of localized prostate cancer. Prostates smaller than 40 mL or those with an anteroposterior diameter of less than 5 cm are best suited for this treatment. During the procedure, the whole gland is treated. They reported that 78% of low-risk patients were disease-free and had negative biopsy results at an actuarial 5-year follow-up (Gelet et al., 2004). Some of the advantages of HIFU are that it is able to be repeated if cancer reappears; it can destroy cancer in targeted areas of the prostate without destroying other areas of the prostate; and it can be given to patients who may not be able to take other forms of prostate treatment such as brachytherapy. Marberger et al reported that HIFU has been used widely in Europe for complete ablation of the prostate, especially in elderly men who are unwilling or unable to undergo radical therapy. For low- or intermediate-risk cancer, the short- and intermediate-term results have been acceptable. Focal use of HIFU should reduce the adverse sexual and urinary side effects of whole gland ablation (Marberger et al., 2008).

8.3 Vascular-targeted photodynamic therapy (VTFT)

VTFT is a minimally invasive ablative treatment for localized prostate cancer and may represent a preferred option for men with low-risk disease who want to balance the risks and benefits of treatment. (Lepor, 2008). VTFT has been used for whole gland ablation of locally recurrent cancer after radiotherapy and for focal ablation of previously untreated cancer. In combination with a new, systemically administered photodynamic agent, laser light is delivered through fibers introduced into the prostate under TRUS. This technique does not heat the prostate but destroys the endothelial cells and cancer by activating the photodynamic agent. Damage to surrounding structures appears to be limited and can be controlled by the duration and intensity of the light. (Marberger et al., 2008).

8.4 TRUS-guided prostate brachytherapy

Brachytherapy is an effective treatment for localized prostate cancer with high patient tolerability and acceptable morbidity outcome data. It delivers a high dose of radiation to a small target volume of tissue, minimizing radiation side-effects to adjacent structures. Brachytherapy is an alternative to radical surgery and external beam radiotherapy and can be delivered in two different ways: permanent seed implants using iodine or palladium seeds or using temporary removable implants with iridium wires. TRUS is essential for accurate imaging guidance to place the radioactive sources into the prostate (Fig. 21). Prostate brachytherapy data has now matured as a treatment with consistent results reported from major centers in the US and Europe (Henry et al., 2010, Battermann et al., 2008).

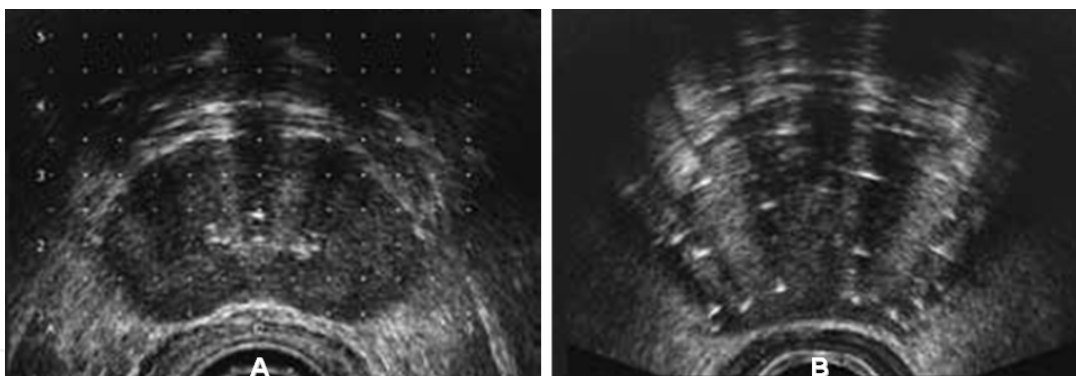


Fig. 21. Prostate brachytherapy. (A) Transrectal ultrasound set-up: transverse image of the prostate with 5mm template overlay. (B) Transverse image of the prostate after seed implant (echogenic areas)

9. Conclusion

One of the major advances that have greatly improved our understanding of prostatic diseases is the development of sonography especially TRUS. It is considered the first imaging modality in diagnosis of prostate diseases. Improvement of the application of the new advances in US for the detection and clinical staging of prostate cancer is promising. TRUS-guided procedures are now widely used in diagnosis and treatment of prostate cancer. Radiologists and urologists should be well trained in the application of these new US techniques and should therefore play an important role in the management of prostate cancer in the future.

10. References

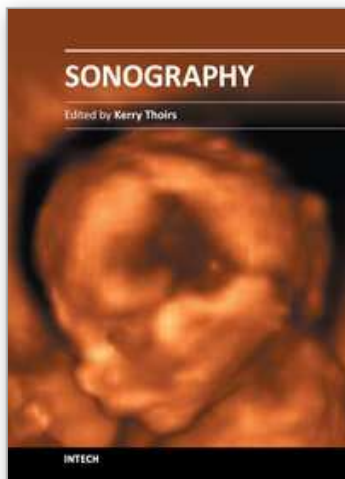
- Abou Yousef M M and Naryana AS (1982). Tran rectal ultrasound in the evaluation of the prostatic size. *J Clin ultrasound*. 10: 275-278.
- Athanasίου A, Tardivon A, Tanter M, Sigal-Zafrani B, Bercoff J, Deffieux T, Gennisson JL, Fink M, Neuenschwander S (2010). Breast lesions: quantitative elastography with supersonic shear imaging--preliminary results. *Radiology*. Jul; 256(1):297-303.
- Babaian RJ, Toi A, Kamoi K, Troncso P, Sweet J, Evans R, Johnston D, Chen M. (2000). A comparative analysis of sextant and an extended 11-core multisite directed biopsy strategy. *JUrol*; 163:152-157.
- Bahn DK, Lee F, Badalament R, Kumar A, Greski J, Chernick M (2002). Targeted cryoablation of the prostate: 7-year outcomes in the primary treatment of prostate cancer. *Urology* Aug; 60(2 Suppl 1):3-11.
- Battermann J, Boon T, Moerland M (2004). Results of permanent prostate brachytherapy, 13 years of experience at a single institution *Radiother Oncol*; 71:23-28
- Benson MC, Whang IS, Pantuck A, Ring K, Kaplan SA, Olsson CA, et al (1992). Prostate specific antigen density: a means of distinguishing benign prostatic hypertrophy and prostate cancer. *JUrol*; 147:815-9.
- Bax J, Cool D, Gardi L, Knight K, Smith D, Montreuil J, Sherebrin S, Romagnoli C, Fenster A (2008). Mechanically assisted 3D ultrasound guided prostate biopsy system. *Med Phys*. Dec ;35(12):5397-410.
- Bercoff J, Tanter M, Fink M (2004). Supersonic shear imaging: a new technique for soft tissue elasticity mapping. *IEEE Trans Ultrason Ferroelectr Freq Control*. Apr;51(4):396-409
- Bogers HA, Sedelaar JP, Beerlage HP, de la Rosette JJ, Debruyne FM, Wijkstra H, Aarnink RG (1999). Contrast enhanced three-dimensional power Doppler angiography of the human prostate: correlation with biopsy outcome. *Urology*; 54: 97-104.
- Brandes D. (1984) prostate gland embryology, anatomy and histology. In: G. Hills. *Uropathology*. Chirchill, Livingstone, New York; 1165-1180.
- Bree RL, De Dreu SE (1998). Contrast enhanced color Doppler of the prostate as an adjunct to gray-scale identification of cancer prior to biopsy. *Radiology*; 209: 418.
- Correas J-M., KHAIROUNE A., Tissier A.-M, Vassiliu V., EISS D., Hélénon O (2011). Trans-rectal quantitative Shear Wave Elastography: application to prostate cancer - A feasibility study. Poster No.: C-1748 Congress: ECR 2011.
- Chen ME, Troncso P, Tang K, Babaian RJ, Johnston D (1999). Comparison of prostate biopsy schemes by computer simulation. *Urology*; 53:951-960.
- Clements R, Gower TK, Griffith GT, Peeling WB (1993) Transrectal ultrasound appearance of granulomatous prostatitis. *Clinic. Radiol*; 47: 174-176.
- Gonder MJ, Soanes WA, Shulman S (1966). Cryosurgical treatment of the prostate. *Invest Urol*. Jan; 3(4):372-8
- Cool D, Sherebrin S, Izawa J, Chin J, Fenster A (2008). Design and evaluation of a 3D transrectal ultrasound prostate biopsy system. *Med Phys*. Oct; 35(10):4695-707.
- Cornud F, Belin X, Fromont G. (1993). Prostate normale. In: *Imaging de la prostate*, H. Nahum ed. *Medecine – Sciences Flammarion*, Paris; 3-18.
- Delmas V, Dauge MC (1991). Embryology of the prostate- current state of knowledge. In: Khoury SCC, Murphy G, Denis L, ed. *Prostate cancer in questions*. Edinburgh, UK: ICI publications;16-17.

- De La Taille A, Benson MC, Bagiella E, Burchardt M, Shabsigh A, Olsson CA, et al (2000). Cryoablation for clinically localized prostate cancer using an argon-based system: complication rates and biochemical recurrence. *BJU Int.* Feb; 85(3):281-6.
- Doble A, Carter SS. (1989) Ultrasonographic findings in prostatitis. *Urol Clin. North Am*; 18, 4.
- Donkol, RH (2010). Imaging in male-factor obstructive infertility. *World J Radiol* 2(5):172-179.
- Egawa S, Wheeler TM, Scardino PT (1991). The sonographic appearances of irradiated prostate cancer. *Brit J Urol*; 172-177.
- Forsberg F, Merton DA, Liu JB et al (1998). Clinical applications of ultrasound contrast agents. *Ultrasonics*; 36: 695–701.
- Frauscher F, Klauser A, Halpern EJ, Horninger W, Bartsch G (2001). Detection of prostate cancer with a microbubble ultrasound contrast agent. *Lancet*; 357: 1849–50.
- Frauscher F, Klauser A, Volgger H, Halpern EJ, Pallwein L, Steiner H, Schuster A, Horninger W, Rogatsch H, Bartsch G (2002). Comparison of contrast enhanced color Doppler targeted biopsy with conventional systematic biopsy: impact on prostate cancer detection. *JUrol*; 167: 1648–52.
- Gelet A, Chapelon JY, Poissonnier L, Bouvier R, Rouvière O, Curiel L (2004). Local recurrence of prostate cancer after external beam radiotherapy: early experience of salvage therapy using high-intensity focused ultrasonography. *Urology*. Apr; 63 (4):625-629.
- Giffiths GJ, Grooks AJR, Roberts EE, Evans KT, Buck AC, Thomas PJ, Peeling WB (1984) Ultrasonic appearance associated with prostatic inflammation: a preliminary study. *Clinic Radiol.*, 35 : 343- 345.
- Hammerer PG, McNeal JE, Stamey TA (1995). Correlation between serum prostate specific antigen levels and the volume of the individual glandular zones of the human prostate. *JUrol* ;153:111- 114.
- Halpern EJ, Rosenberg M, Gomolla LG (2001). Contrast enhanced sonography of the prostate. *Radiology*; 219: 219–25.
- Hamper UM, Sheth S (1993). Prostate ultrasonography. *Semin roentg*; 28, 1: 57 – 73.
- Henry AM, Al-Qaisieh B, Gould K, Bownes P, Smith J, Carey B, Bottomley D, Ash D (2010). Outcomes following iodine-125 monotherapy for localized prostate cancer: the results of leeds 10-year single-center brachytherapy experience. *Int J Radiat Oncol Biol Phys.* Jan 1; 76(1):50-56.
- Hodge KK, McNeal JE, Terris MK, Stamey TA (1989). Random systematic versus directed ultrasound guided transrectal core biopsies of the prostate. *JUrol* ;142:71-75.
- Hricak H (1990). The prostate gland. In: Hricak H, Carrington BM (eds.). *MRI of the pelvis. A text atlas.* California Martin Dunitz:
- Inahara M, Suzuki H, Nakamachi H, Kamiya N, Shimbo M, Komiya A, Ueda T, Ichikawa T, Akakura K, Ito H (2004). Clinical evaluation of transrectal power doppler imaging in the detection of prostate cancer. *Int Urol Nephrol* ;36(2):175-80.
- Ismail M, Petersen RO, Alexander AA, Newschaffer C, Gomella LG (1997). Color Doppler imaging in predicting the biologic behavior of prostate cancer: correlation with disease-free survival. *Urology*; 50: 906–12.
- Jacobs S, C (1983). Spread of prostatic cancer to bone. *Urology* 21 : 337.
- Klauser A, Koppelstaetter F, Berger AP, Horninger W, Lorenz A, Frauscher F (2003). Real-time elastography for prostate cancer detection: preliminary experience. *Radiology*; 229 (Suppl): 1395

- Konig K, Scheipers U, Pesavento A, Lorenz A, Ermert H, Senge T (2005). Initial experiences with real-time elastography guided biopsies of the prostate. *JUrol*; 174: 115–17.
- Lee F, Littrup PJ, Torp-Pedersen ST, Mettlin C, McHugh TA, Gray JM, Kumasaka GH, McLeary RD (1988) Prostate cancer: Comparison of transrectal US and digital rectal examination for screening. *Radiology*; 168 : 389- 394.
- Lepor H (2008). Vascular targeted photodynamic therapy for localized prostate cancer. *Rev Urol. fall*; 10(4): 254–261.
- Liang K, Rogers AJ, Light ED, Von Allmen D, Smith SW (2010). Simulation of autonomous robotic multiple-core biopsy by 3D ultrasound guidance. *Ultrason Imaging. Apr*; 32(2):118-27.
- Littrup PJ, Klein RM, Gross ML, Sparschu RA, Segel MC, Zingas AP (1995). Color Doppler of the prostate: histologic and racial correlations. *Radiology*; 197: 365
- Lowsley OS (1912). The development of human prostate gland with reference to the development of other structures of the neck of the urinary bladder. *Am J Anat*, 13: 299-349.
- Marberger M, Carroll PR, Zelefsky MJ, Coleman JA, Hricak H, Scardino PT, Abenham LL (2008). New treatments for localized prostate cancer. *Urology. Dec*; 72(6 Suppl):S36-43.
- Mc Lanhin AP, Saltzstein SL, McCullough, DL and Gittes RF (1976) prostatic carcinoma: Incidence location of unsuspected lymphatic metastasis. *J Urol*. 115 – 89.
- Mc Neal JE (1968). Regional morphology and pathology of the prostate. *Am J Clin Pathol*, 49: 347 – 357.
- Mc Neal JE (1983). The prostate gland; morphology and pathology. *Monogr. Urol.*, 4: 5 -13.
- Mc Neal JE (1988). Normal anatomy of the prostate and changes in benign prostatic hypertrophy and carcinoma. *Semin US CT, MRI*, 9: 329 -334.
- Muldoon L and Resnick ML. Result of ultrasonography of the prostate (1989). *Urol Clin North Am*, 16, 4: 693 – 701.
- Myers RP, Geollner JR, Cahil DR (1987) Prostate shape, external striated urethral sphincter and radical prostatectomy: The apical dissection. *JUrol*, 138: 543-548.
- Naughton CK, Miller DC, Mager DE, Ornstein DK, Catalona WJ (2000). A prospective randomized trial comparing 6 versus 12 prostate biopsy cores: impact on cancer detection. *JUrol.*; 164:388-392.
- Naryan P, Foster L (1991). The rule of intravenous urography and magnetic resonance imaging in the evaluation of men with symptomatic benign prostatic hyperplasia. *Probl urol*, 5, 3: 369-379.
- Newman JS, Bree RL, Rubin JM (1995). Prostate cancer: diagnosis with color Doppler sonography with histologic correlation of each biopsy site. *Radiology*; 195: 86–90.
- Ophir J, Cespedes I, Ponnekanti H, Yazdi Y, Li X (1991). Elastography: a quantitative method for imaging the elasticity of biological tissues. *Ultrason Imaging*; 13:111–34.
- Onik GM, Cohen JK, Reyes GD, Rubinsky B, Chang Z, Baust J (1993). Transrectal ultrasound-guided percutaneous radical cryosurgical ablation of the prostate. *Cancer. Aug 15*; 72(4):1291-9.
- Patel U, Rickards D (2002). *Handbook of Transrectal Ultrasound and Biopsy of the Prostate*. Martin.Dunitz Ltd, London.
- Richards D (1992). Transrectal ultrasound, 1992. *Brit JUrol*; 69, 449-465.
- Rifkin MD, Dahnert W, Kurtz AB (1990). State of the art: endorectal sonography of the prostate gland. *AJR*; 154:691-700

- Rifkin MD (1997). *Ultrasound of the Prostate*. 2nd edn. Philadelphia, PA: Lippincott-Raven.
- Rifkin MD, Sudakoff GS, Alexander AA (1993). Prostate: techniques, results, and potential applications of color Doppler US scanning. *Radiology*; 186: 509–13.
- Scardino PT, Shinohara K, Wheeler TM, Carter SS (1989). Staging of prostate cancer: Value of ultrasonography. *Urol Clin North AM*; 16, 713-733.
- Shabsigh R, Kadmon D, Fishman IJ (1989). Ultrasonographically guided transperineal prostate biopsy in patients with suspicious glands and previously negative digitally guided biopsies. *J Endourol.*, 3: 185.
- Shen F, Shinohara K, Kumar D, Khemka A, Simoneau AR, Werahera PN, Li L, Guo Y, Narayanan R, Wei L, et al (2008). Three-dimensional sonography with needle tracking: role in diagnosis and treatment of prostate cancer. *JUltrasound Med. Jun*; 27(6):895-905.
- Shinohara K, Scardino PT, Carter ST, Wheeler TM (1989). Pathological basis of the sonographic appearance of the normal and malignant prostate. *Urol Clin North AM*; 16, 4: 675-691.
- Sohlberg OE, Chetner M, Ploch N, Brawer MK (1991). Prostatic abscess after transrectal ultrasound guided biopsy. *JUrol*; 146, 420-422.
- Takahashi H, Ouchi T. The ultrasonic diagnosis in the field of urology (1963). *Proc Jap Soc Ultrasonics Med*; 3:7.
- Terris MK, McNeal JE, Stamey TA (1990). Invasion of the seminal vesicles by prostatic cancer: Detection by transrectal sonography. *AJR*; 155; 811-815.
- Terris MK, and Stamey TA (1991). Determination of prostatic volume by transrectal ultrasound. *JUrol*, 145: 984-987.
- Wasserman NF, Kapoor DA, Hildebrandt WC, et al (1992) Transrectal ultrasound in evaluation of patients after radical prostatectomy. *Radiology*; 185; 361-372.
- Watanabe H, Igari D, Tanahasi Y, Harada K, Saito M. Development and application of new equipment for transrectal ultrasonography. *JClin Ultrasound*. 1974; 2:91-98.
- Weaver RP, Noble MJ, Weigle JW (1991). Correlation of ultrasound guided and digitally directed transrectal biopsies of palpable prostatic abnormalities. *J Urol.*; 145:516-518.

IntechOpen



Sonography

Edited by Dr. Kerry Thoires

ISBN 978-953-307-947-9

Hard cover, 346 pages

Publisher InTech

Published online 03, February, 2012

Published in print edition February, 2012

Medical sonography is a medical imaging modality used across many medical disciplines. Its use is growing, probably due to its relative low cost and easy accessibility. There are now many high quality ultrasound imaging systems available that are easily transportable, making it a diagnostic tool amenable for bedside and office scanning. This book includes applications of sonography that can be used across a number of medical disciplines including radiology, thoracic medicine, urology, rheumatology, obstetrics and fetal medicine and neurology. The book revisits established applications in medical sonography such as biliary, testicular and breast sonography and sonography in early pregnancy, and also outlines some interesting new and advanced applications of sonography.

How to reference

In order to correctly reference this scholarly work, feel free to copy and paste the following:

Ragab Hani Donkol and Ahmad Al Nammi (2012). Prostate, Sonography, Dr. Kerry Thoires (Ed.), ISBN: 978-953-307-947-9, InTech, Available from: <http://www.intechopen.com/books/sonography/prostate>

INTECH
open science | open minds

InTech Europe

University Campus STeP Ri
Slavka Krautzeka 83/A
51000 Rijeka, Croatia
Phone: +385 (51) 770 447
Fax: +385 (51) 686 166
www.intechopen.com

InTech China

Unit 405, Office Block, Hotel Equatorial Shanghai
No.65, Yan An Road (West), Shanghai, 200040, China
中国上海市延安西路65号上海国际贵都大饭店办公楼405单元
Phone: +86-21-62489820
Fax: +86-21-62489821

© 2012 The Author(s). Licensee IntechOpen. This is an open access article distributed under the terms of the [Creative Commons Attribution 3.0 License](#), which permits unrestricted use, distribution, and reproduction in any medium, provided the original work is properly cited.

IntechOpen

IntechOpen